Front. Environ. Sci. Eng. 2021, 15(4): 54
https://doi.org/10.1007/s11783-020-1346-6

RESEARCH ARTICLE

Sustainable wood-based nanotechnologies for photocatalytic degradation of organic contaminants in aquatic environment

Xinyi Liu [1,#], Caichao Wan (✉)[1,4,#], Xianjun Li[1], Song Wei[1], Luyu Zhang[1], Wenyan Tian[1], Ken-Tye Yong[3], Yiqiang Wu[1], Jian Li (✉)[2]

1 College of Materials Science and Engineering, Central South University of Forestry and Technology, Changsha 410004, China
2 Material Science and Engineering College, Northeast Forestry University, Harbin 150040, China
3 School of Electrical and Electronic Engineering, Nanyang Technological University, Singapore 639798, Singapore
4 Yihua Lifestyle Technology Co., Ltd, Huaidong Industrial Zone, Lianxia Town, Chenghai District, Shantou 515834, China

HIGHLIGHTS

- Wood and its reassemblies are ideal substrates to develop novel photocatalysts.
- Synthetic methods and mechanisms of wood-derived photocatalysts are summarized.
- Advances in wood-derived photocatalysts for organic pollutant removal are summed up.
- Metal doping, morphology control and semiconductor coupling methods are highlighted.
- Structure-activity relationship and catalytic mechanism of photocatalysts are given.

ARTICLE INFO

Article history:
Received 24 March 2020
Revised 16 June 2020
Accepted 28 June 2020
Available online 9 November 2020

Keywords:
Wood
Nanocatalysts
Photodegradation
Organic contaminants
Composites

GRAPHIC ABSTRACT

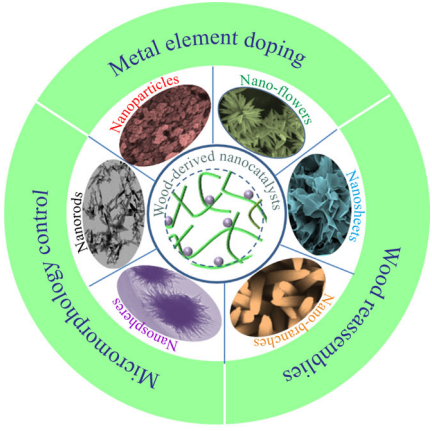

ABSTRACT

Wood-based nanotechnologies have received much attention in the area of photocatalytic degradation of organic contaminants in aquatic environment in recent years, because of the high abundance and renewability of wood as well as the high reaction activity and unique structural features of these materials. Herein, we present a comprehensive review of the current research activities centering on the development of wood-based nanocatalysts for photodegradation of organic pollutants. This review begins with a brief introduction of the development of photocatalysts and hierarchical structure of wood. The review then focuses on strategies of designing novel photocatalysts based on wood or its recombinants (such as 1D fiber, 2D films and 3D porous gels) using advanced nanotechnology including sol-gel method, hydrothermal method, magnetron sputtering method, dipping method and so on. Next, we highlight typical approaches that improve the photocatalytic property, including metal element doping, morphology control and semiconductor coupling. Also, the structure-activity relationship of photocatalysts is emphasized. Finally, a brief summary and prospect of wood-derived photocatalysts is provided.

1 Introduction

The fast development of economy and society brings a major challenge: pollution. In the past few decades, the rapid growth of industrial activities has caused poor water quality and serious damage to ecosystem (Osibanjo et al., 2011; Giri and Singh; 2014). While destroying the aquatic environment, such pollution has simultaneously caused

✉ Corresponding authors
E-mail: wancaichaojy@163.com (C.Wan); nefulijian@163.com (J.Li)
#These authors contributed equally to this work and are considered co-first authors.

great harm to humans and other organisms. Organics (such as dye and pesticides) are typical pollutants in water environment. For example, dieldrin, a famous organochloride, was produced in 1948 and is known as a high-efficiency insecticide to protect crops from insect pests. Because of high toxicity, carcinogenicity and bioaccumulation, this organochloride had been banned in 2001 by international conventions (Kamata et al., 2010). Polychlorinated biphenyls, which are mainly used as insulating liquids in power transformers and capacitors, can induce cancer (Huang et al., 2011). According to the United Nations Environment Programme (UNEP), 80% of the world's wastewater is directly discharged into the water environment without treatment in 2015. Worldwide, removing organic contaminants from wastewater remains a major challenge. Solving this issue is of great significance to the sustainable development of the world (Hao et al., 2019). As is well known, solar energy is an inexhaustible source of clean energy, and photocatalytic technology possesses many advantages over traditional methods (for instance, adsorption (Kuang et al., 2019), biodegradation (Ren et al., 2018) and direct burning) in dealing with organic pollution, e.g., moderate conditions, no secondary pollution (Zazouli, 2019; Ebrahimzadeh et al., 2020b; Shirzadiahodashti et al., 2020), high degradation efficiency and low energy consumption (Moustakas et al., 2014; Zhao et al., 2016). Zinatloo-Ajabshir et al. (2017) reported Nd_2O_3 nanostructure that was prepared by an easily-operated Schiff alkaline hydrothermal approach. The material can fastly decompose chrome black T dyes in water. Safariamiri et al. (2017) employed a combined solvent-free solid-phase method and heat treatment to prepare Dy_2O_3 nanoparticles that can photodegrade rhodamine B (RhB). Ebrahimzadeh et al. (2020a) prepared $Fe_3O_4/SiO_2/ZnO\text{-}Pr_6O_{11}$ by virtue of sonochemical technology in the presence of carbohydrates. This hybrid is capable to quickly photodegrade organic substances. Therefore, these studies have verified that photocatalytic degradation is one of the most effective pathways to address organic wastewater. However, the photocatalytic method still has some shortcomings, like the low-efficiency exploitation of visible light because of the wide band gap for common natural photocatalysts (Sun, 2014), low adsorption capacity for hydrophobic pollutants, nonuniform distribution in water suspensions and difficult recovery of powder-like photocatalysts from water.

In 1972, Fujishima and Honda (1972) reported the photolysis of hydrogen on TiO_2 electrodes for the first time. In 1976, Carey et al. (1976) found that TiO_2 materials could effectively catalyze the degradation of organic matter in water under ultraviolet (UV) irradiation. Since then, photocatalytic technology has received broad attention. After decades of development, researchers have synthesized multifarious types of photocatalytic materials, such as metal compounds (Tian et al., 2014), nitrides (Wang et al., 2018), and organic photocatalysts (Wang et al., 2015a), with the help of various approaches that typically include hydrothermal synthesis (Ide et al., 2016), sol-gel processing (Palanisamy et al., 2013), and magnetron sputtering (Cojocaru et al., 2011), which have greatly promoted the advancement of photocatalytic technology. TiO_2 has become one of the most intensively studied and applied photocatalysts due to high photocatalytic activity, high chemical stability, nontoxicity, lack of secondary pollution and low cost (Jiang et al., 2011; Paramasivam et al., 2012). The photocatalytic mechanism of TiO_2 includes three procedures (Guo et al., 2019). First, under the condition of the light absorption exceeding the band gap energy of the photocatalyst, an electron–hole pair is formed. Secondly, the pair tends to dissociate, leading to the formation of free electron and hole, and then they migrate to the reactive surface. In final, these free electrons and holes are combined with adsorbed molecules, resulting in the occurrence of photoreduction/photooxidation. To notably improve the photocatalytic activity and recyclability of TiO_2-based photocatalysts, restraining the recombination of charge carriers and reducing the band gap play important roles. The methods like doping, integration, surface sensitization and modification are involved. Besides, it is useful to further increase the recoverability of nano-TiO_2 by integrating this nanomaterial with various porous macroscopic materials (such as gels, films, and foams) (Yu and Xu, 2007; Khojasteh et al., 2019). Therefore, TiO_2 has become a reliable material in the treatment of environmental pollution. TiO_2 is a large bandgap semiconductor with three kinds of common crystal structures: rutile (3.0 eV), anatase (3.2 eV) and brookite titanium (Linsebigler et al., 1995; Yu and Xu, 2007; Zhang et al., 2014), as illustrated in Fig. 1.

ZnO is also a popular semiconductor material with excellent photocatalytic properties and has been extensively studied due to its advantages of nontoxicity, high efficiency and low cost. The photodegradation mechanism of ZnO has been proven to be similar to that of TiO_2, and this material appears to be a suitable substitute for TiO_2 (Chong et al., 2010). At room temperature, the forbidden band width of ZnO is 3.2 eV, absorbing UV light with a wavelength of less than 380 nm and exciting electrons in the valence state to produce photogenerated electron-hole pairs (Zhang et al., 2015). Moreover, high-activity radical groups (like $\cdot OH$ and $\cdot O_2^-$) with quite strong redox ability are formed, thereby decomposing organic pollutants in aquatic environment.

The single-component photocatalysts for degrading organic pollutants mainly exist in powder form and thus have a strong tendency to agglomerate. On the one hand, in the actual application process, only superficial photocatalysts can absorb light energy and adsorb pollutants, and the activity of inner photocatalysts is difficult to exert, resulting in low photocatalytic efficiency. On the other

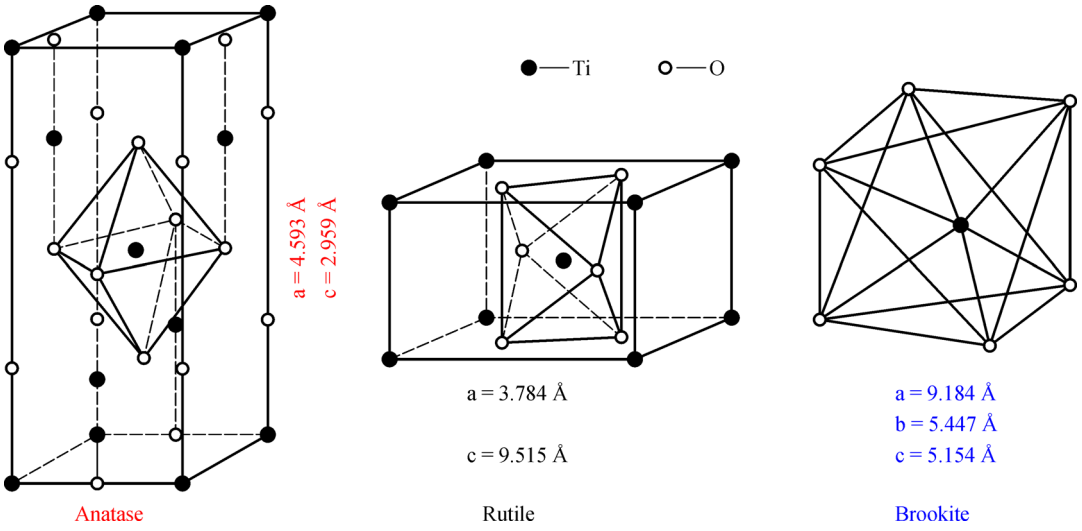

Fig. 1 Three kinds of common TiO_2 crystals.

hand, powders are easily dispersed, and these dispersions not only need a complicated recycling, but also cause secondary pollution. The integration of photocatalytic materials with substrates can solve the above problems by firmly immobilizing the nanomaterials (Zhang et al.,2017; Zhou et al., 2018). Depending on their sources, these substrates can be divided into natural and synthetic substrates. For natural substrates, for instance, Huang et al. (2008) deposited Pt-modified TiO_2 on natural zeolite by sol-gel and photoreduction deposition methods, and the composite could be used to degrade methyl orange (MO). Wang et al. (2015b) employed facile methods to create Cu_2O nanoparticles on graphene oxide/chitin films, and there is a strong interaction between graphene oxide and these natural substances (e.g., chitin and plant extracts (Khojasteh et al., 2019). The visible-responsive photocatalysts are capable to fastly degrade dyes. For the use of artificial substrates, for example, Iguchi et al. (2003) grew TiO_2 photocatalysts onto inorganic fiber substrates, and the photocatalysts are capable to degrade acetaldehyde under UV radiation. Janbandhu et al. (2019) reported glass-based CdS/TiO_2 heterojunction photocatalysts for the degradation of indigo carmine dyes. Zhao et al. (2019) improved the photocatalytic degradation of RhB by doping Ag_2S quantum dots with flower-like SnS_2. In addition, other representative substrates including cotton fabrics, bentonite (Gautam et al., 2017), activated carbon (Hu et al., 2017; Gusain et al., 2020), multiwalled carbon nanotubes (Lu and Astruc, 2020), porous polymers (Wong et al., 2016; Byun and Zhang, 2020) and metal-organic frameworks (Meng et al., 2018; Yamashita et al., 2018) have been adopted for the development of novel and high-performance photocatalysts. Among these substrates, wood is especially alluring because it not only has a large surface area, high porosity, low density, and excellent environmental friendliness but also possesses abundant oxygen-containing groups and vertical channels along its growth direction (Fig. 2). These features are beneficial for the adhesion and growth of nanomaterials, resulting in high loading and strong stability along with superior photodegradation properties toward organic pollutants (Moon et al., 2011; Shi et al., 2014). Thus, wood-derived photocatalysts have been extensively studied in recent years.

Some excellent review papers on the preparation, characterization and photodegrading organic contaminants have been published (Devi and Kavitha, 2013; Zangeneh et al., 2015). Most of these reviews primarily summarized the prominent works emerging in given a period, the preparation and photocatalytic applications of a specific kind of material (such as TiO_2 and ZnO), or particular modification methods. Nevertheless, review articles focused on the application of wood-based nanotechnologies for the photodegradation of organic contaminants have not yet been fully realized. Therefore, it is timely to review the instructive topic to summarize the recent advances and, more importantly, to provide a systematic understanding of the advantages of the use of wood or its assemblies for photocatalytic degradation. In this critical review, we will focus on the preparation strategies, structural advantages, physicochemical features, and photocatalytic activity of wood-derived photocatalysts and their applications for removing organic pollutants from the water environment. Some typical strategies for photocatalytic activity improvement are highlighted, including metal element doping, micromorphology control and semiconductor coupling. Finally, a brief summary and prospect of wood-derived photocatalysts is put forward.

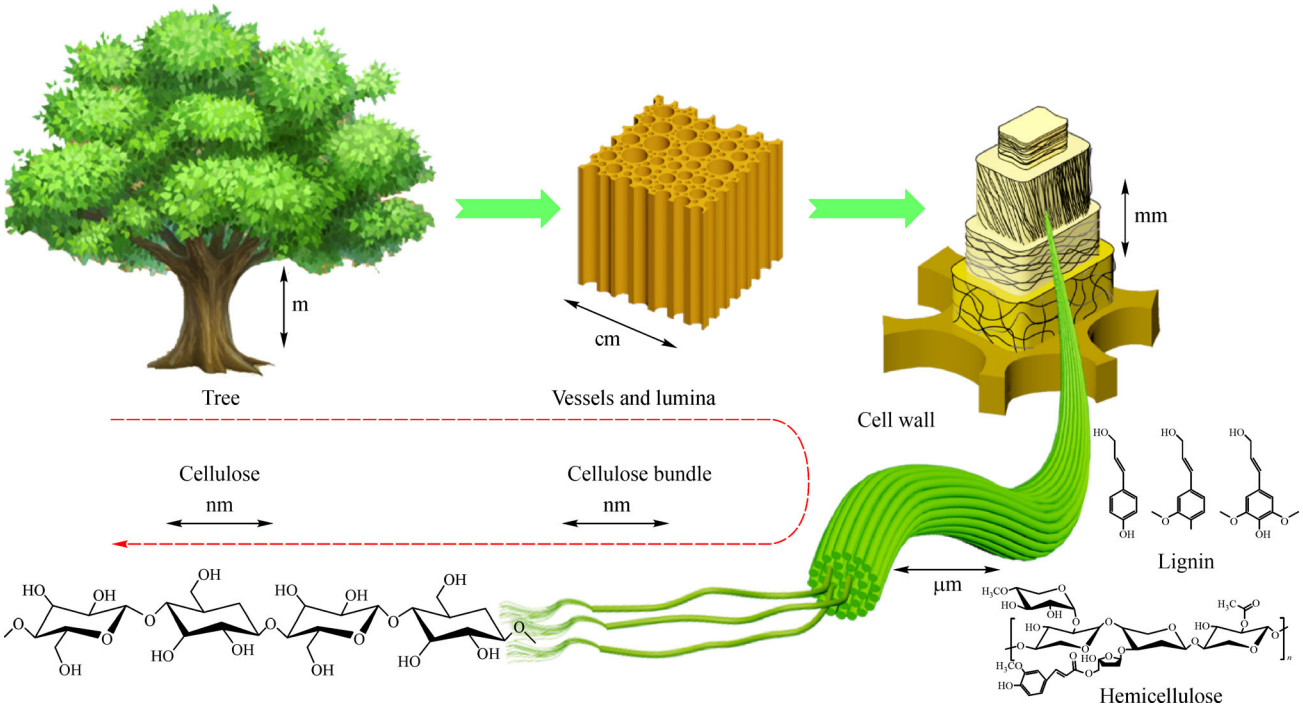

Fig. 2 Hierarchical structure of wood: from tree to cellulose molecule chains (from m to nm).

2 Preparation strategies of wood-derived photocatalysts

Generally, there are two main ways to prepare wood-derived photocatalysts: 1) wood or its derivatives directly participate in the synthetic reaction of photocatalytic active substances; or 2) wood or its derivatives are combined with synthesized photocatalytically active substances. Representative synthetic strategies of wood-derived photocatalysts are presented below (Fig. 3).

2.1 Sol-gel method

The sol-gel technology aims at forming a stable transparent sol system with the help of hydrolysis and condensation reactions (Akpan and Hameed, 2010). The subsequent aging induces the polymerization of colloidal particles and the formation of three-dimensional (3D) network of gels. The reaction steps are presented as follows (Macwan et al., 2011):

1) Solvation: a hydrate species $[M\cdot(H_2O)_n]^{z+}$ is formed due to the interaction between M^{z+} (metal salt cation) and water molecules. The hydrate can release H^+:

$$[M\cdot(H_2O)_n]^{z+} \rightarrow [M\cdot(H_2O)_{n-1}(OH)]^{(z-1)+} + H^+ \quad (1)$$

2) Hydrolysis: $M(OR)_n$ (R indicates an alkyl group) reacts with water, leading to the formation of $M(OH)_n$:

$$M(OR)_n + xH_2O \rightarrow M(OH)_x(OR)_{n-x} + xROH \quad (2)$$

3) Polycondensation: this process can be divided into water loss polycondensation and alcohol loss polycondensation, dependent on the type of removed molecule:

Water loss polycondensation :

$$M\text{-}OH + HO\text{-}M \rightarrow M\text{-}O\text{-}M + H_2O \quad (3)$$

Alcohol loss polycondensation :

$$M\text{-}OR + HO\text{-}M \rightarrow M\text{-}O\text{-}M + ROH \quad (4)$$

The merits of this method include low equipment requirements, simple process, easily controlled reaction, diversified product forms and high purity. The sol-gel way can be adopted to prepare organic-inorganic hybrids at a low temperature, to avoid the degradation of organic matters at high temperature Typically, many researchers have used this method to prepare TiO_2 photocatalytic composites (Su et al., 2004; Wang et al., 2011a). Generally, titanates (such as tetrabutyl titanate) are used as raw materials, and they are added to a specific solvent (such as ethanol) under stirring conditions. After adjusting its pH value by nitric acid or glacial acetic acid, the anti-solvent (like water) is dropped into the titanate solution under stirring to form a sol. Besides, a heating treatment is capable of accelerating the gelation process (Gezimati et al., 1996; Wan et al., 2016).

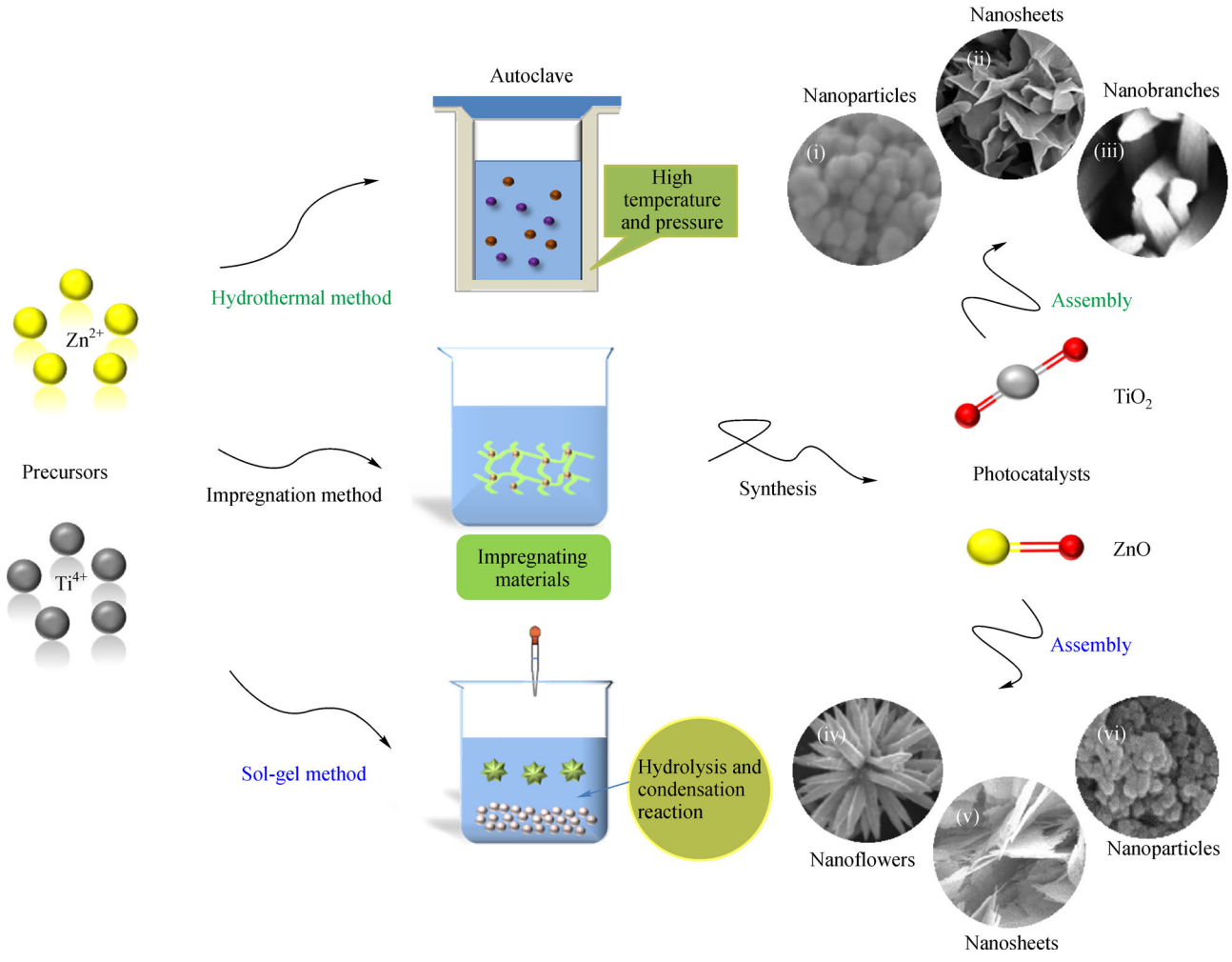

Fig. 3 Schematic diagram of representative synthetic methods of photocatalytic materials with different micromorphologies. (i–vi) SEM images of TiO_2 and ZnO with different micromorphologies (i. Adapted from Wu et al. (2014) with the permission of the Elsevier; ii. Adapted from Gao et al. (2015) with the permission of the Elsevier; iii. Adapted from Wang et al. (2011b)with the permission of the Royal Society of Chemistry; iv. Adapted from Wahab et al. (2007) with the permission of the Elsevier; v. Adapted from Meng et al. (2015) with the permission of the Elsevier; vi. Adapted from Hong et al. (2015) with the permission of the Elsevier).

2.2 Hydrothermal method

The hydrothermal method is a liquid-phase chemical technique and conducted in a special closed reactor (such as autoclave). By heating and pressurizing the system (or with the help of autogenous vapor pressure), high-temperature and high-pressure reaction conditions are created. The hydrothermal method is an ideal approach for inorganic synthesis and material processing by dissolving and recrystallizing normally insoluble materials (Ratha and Rout, 2013; Zhang et al.,2020).

The general procedures for hydrothermal synthesis consist of the following four steps: 1) selecting reaction precursors and determining the amount ratio of precursors; 2) determining the order of addition of precursors and stirring wet materials; 3) loading and sealing the autoclave and then placing it into an oven; and 4) selecting the reaction temperature, time and state (static or dynamic crystallization). Compared with other methods, the hydrothermal method has the following merits: 1) can directly yield well-crystalline products without complex post-treatment; 2) the crystal form and morphology of the products are related to hydrothermal conditions (such as temperature, time and pH); 3) the crystal grain linearity is moderately adjustable; 4) the reaction has low energy consumption and high output; and 5) the process is simple and mild (Tomita et al., 2006; Wei et al., 2019). Apart from these merits, more importantly, the hydrothermal method can promote the assembly of photocatalytic substances on the surface of wood (Li and Xu, 2010). Taking TiO_2 as an example, the representative synthetic procedures can be briefly summarized as follows: tetrabutyl titanate (TBOT) is first dissolved into anhydrous ethyl alcohol and then transferred to an autoclave. The wood sample is placed into

the above solution, and then, the reactor is heated at a specific temperature and pressure. After heating, the product is rinsed and dried.

2.3 Magnetron sputtering

As a representative physical vapor deposition technique, magnetron sputtering relies on the collision between injected gas and targets. The accelerated ionized gas collides with the target atom, and thus the target atoms are sputtered out (Wang et al., 2016; Singh et al., 2017).

Since the advent of magnetron sputtering, this method has achieved fast development and wide application. Its merits mainly include fast deposition rate, low temperature, small damage to products, high bonding strength and purity and controllable thickness (Maurya et al., 2014). Thus, this method has been used to prepare film-like photocatalytic materials (Heo et al., 2005). Taking TiO_2-based photocatalysts as an example, substrates are first cleaned in an ultrasonic bath and subsequently introduced to a vacuum system. A TiO_2 disc with specific specifications is applied as the sputtering target. High-purity argon is a common sputtering and reaction gas. Finally, a TiO_2 film is deposited, and after deposition, TiO_2-based photocatalysts are acquired.

2.4 Impregnation method

The impregnation method involves immersing substrate materials into soluble compound solutions containing active components (namely, main and auxiliary catalytic components) and then separating the residual liquid from the substrates after contact for a certain time. Therefore, the active components are attached to the substrates in the form of ions or compounds, which is known as impregnation. The capillary pressure generated by the surface tension promotes the penetration of liquid into the porous substrates. For the purpose of increasing the amount or depth of impregnation, it is sometimes possible to evacuate the air in the substrates in advance (i.e., the vacuum impregnation method). Moreover, it is also effective to raise the temperature of impregnation liquids (namely reducing the viscosity) and to accelerate the agitation rate.

The impregnation method has the following advantages: 1) the method is suitable for various shapes and sizes of substrates, and the formation steps of the catalysts are rapid and facile; 2) suitable substrates can provide structural characteristics required for the catalysts; and 3) active matters is distributed on the surface of substrates, and thus the utilization rate is high and the cost is relatively low, which are particularly important features for precious metal catalysts such as platinum, palladium and rhodium. Due to these merits, the impregnation method is extensively considered to be a simple and economical method that is quite appropriate for the synthesis of substrate-supported catalysts, especially for precious metal-based catalysts such as Pt/TiO_2 photocatalysts (Zou et al., 2004) and direct Z-type $LaCoO_3$/g-C_3N_4 heterojunction photocatalysts (Jin et al., 2019).

2.5 Other synthetic methods

There are still some other interesting synthetic ways for wood-derived photocatalysts. For example, Rajeswari et al. (2017) used a solution dispersion blending method to create cellulose acetate-polyurea membranes integrated with nano-ZnO. Kemell et al. (2005) first reported TiO_2/cellulose hybrids synthesized by the atomic layer deposition method. Furthermore, a CdS/regenerated cellulose hybrid membrane was created by Ke et al. (2009) by virtue of the chemical precipitation method (namely, soaking a regenerated cellulose membrane in a mixed solution of $CdCl_2$ and Na_2S).

3 Wood-based photocatalysts for removal of organic pollutants

Organic pollutants in aquatic environmental are a major concern, and the degradation of organic pollutants is an important application area of photocatalysts. In general, powder-like photocatalysts are easily agglomerated and have a low adsorption capacity and thus do not easily adsorb contaminants. In addition, powders are prone to produce secondary pollution. Wood-derived photocatalytic materials not only make full use of the characteristics of wood or its derivatives, but also have improved photocatalytic properties compared to those of powder-like photocatalysts because of their high dispersion and stability. Most importantly, wood-derived photocatalysts simultaneously achieve adsorption and photodegradation, i.e., they are able to degrade organic pollutants into nontoxic small molecules under light irradiation while retaining excellent adsorption capacity. The degradation of organic pollutants by wood-derived photocatalysts can be divided into three steps: 1) organic contaminants are adsorbed by wood-derived photocatalytic materials; 2) the photocatalysts absorb light energy, inducing the formation of electron-hole pairs; and 3) these electron-hole recombination migrate to the photocatalyst surface to react with organic matters and the contaminants are completely degraded via a multistep process. The photocatalytic mechanism of wood-derived photocatalysts is illustrated in Fig. 4. The section will focus on the physicochemical features and photocatalytic activity of wood-derived photocatalytic materials for the application of removal of organic contaminants. Table 1 summarizes representative wood-derived photocatalysts from the recent literature.

In the process of photocatalysis, holes and electrons are the products of absorption of light energy. Also, their separation efficiency determines the photocatalytic efficiency. It is worth mentioning that constructing semicon-

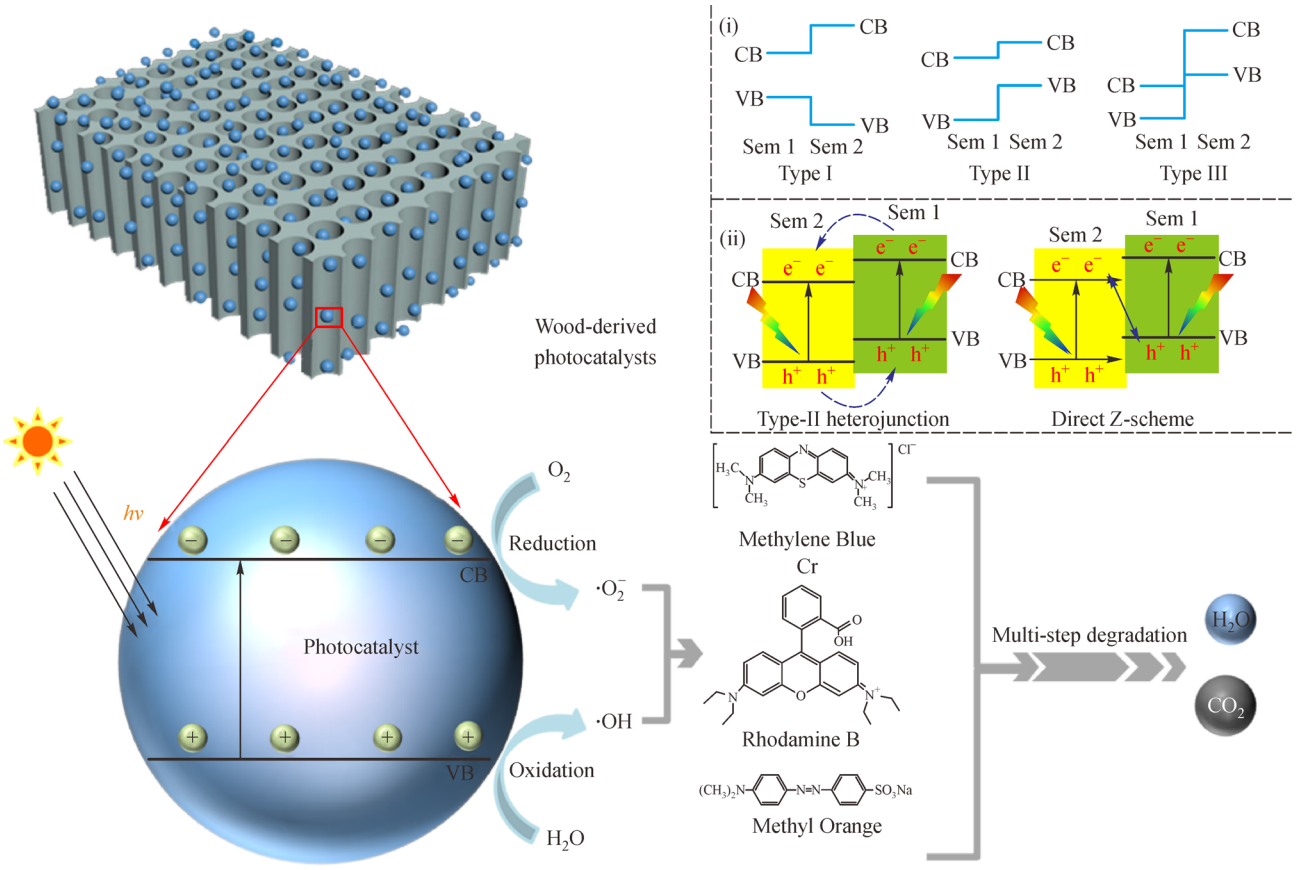

Fig. 4 Schematic representation of the photocatalytic mechanism of wood-derived photocatalysts (typically including wood-supported TiO_2 or ZnO). (i) Construction of semiconductor heterostructures (type I, II and III) to improve the efficiency of photoinduced charge separation; (ii) electron hole transfer for type II and direct Z-type heterojunctions (i. Adapted from Wang et al. (2013). with the permission of the publishes; ii. Adapted from Xu et al. (2018) with the permission of the Elsevier).

ductor heterostructures is an effective way. The heterojunction is composed of two semiconductors with a staggered-band configuration. According to the bandgaps and electronic affinity, there are three cases: type-I, -II and-III (Wang et al., 2013). As presented in Fig. 4(i), for type I, the conduction band (CB) of Sem. I is lower while its valence band (VB) is higher. Thus, the electrons and holes move to the CB and VB of Sem. I, which is not conducive to separating electron-hole pairs. For type III, the overlapped band gaps play a negative role in the separation of pairs. In contrast, the construction of type II is beneficial for the enhancement of photocatalytic efficiency. As shown in Fig. 4(ii), the electrons move to Sem. II owing to the higher CB of Sem. I. On the contrary, the holes conduct a reverse migration. As a result, the reduction reaction occurs on Sem. II due to the existence of electrons, while the oxidation reaction will happen on Sem. I because of the presence of holes (Bai et al., 2015). This phenomenon heightens the energy conversion efficiency (Gao et al., 2016; Xia et al., 2017; Xu et al., 2018).

Z-type photocatalytic system is also an effective heterostructure. Its two-step photoexcitation is like the English letter "Z." Typically, the higher reaction activity of electrons in the Sem. I CB and holes in the Sem. II VB of are retained. The lower activity of electrons in the Sem. II CB and holes in the Sem. I VB recombine. Therefore, Z-type system also has a superior redox power (Xu et al., 2018; Gu et al., 2020).

3.1 Photocatalytic activity improved by metal element doping

The photocatalytic activity of photocatalysts is restricted by many factors. The doping of metal elements is one of the most important methods for activity improvement. Metal element doping (typically including Ag (Liu et al., 2015), Fe (Singh et al., 2011; Tonda et al., 2014), Cu (Sathishkumar et al., 2011) and other elements (Khojasteh et al., 2016; Fan et al., 2020; Fujiwara et al., 2020) can form doping energy levels and change the electronic structure (Han et al., 2015; Xiong et al., 2016), because the electronic structure can be altered by compositing the atomic orbital of the dopant with the original molecular orbitals of the photocatalysts (Shi et al., 2017). By doping,

the energy levels of Zn-MoS_2 and Fe-MoS_2 allow the electron transfer under lower energies (Fig. 5(a)). Ag is a famous doping element. Yu et al. (2012) prepared TiO_2/Ag sponge-like composites using natural cellulose (a typical component in the cell wall of wood) as the template via a sol-gel method (Fig. 5(b)). X-ray diffraction (XRD) pattern confirms the existence of anatase structure (Fig. 5(c)) with a higher activity among various common TiO_2 crystals (such as rutile and brookite TiO_2) (Li et al., 2014; Zhang et al.,2014). In Fig. 5(d), the sponge-like composites achieve a slight adsorption capacity for aqueous salicylic acid (~5%) within 30 min. As the Ag content is 5.1 wt%, the salicylic acid degradation rate reaches 97.8%. When the Ag content further increases to 8.3 wt%, the salicylic acid degradation rate decreases to 70.9%, possibly because the composite possesses the lowest specific surface area and limits the loading of TiO_2.

Xuan et al. (2018) adopted a sol-gel technology to prepare a SiO_2/TiO_2 hybrid film doped with ferric ions (labeled as Fe^{3+} -doped STCF) on the wood surface. The SEM image (Fig. 6(a)) shows that the composite film only covers the wood surface and does not penetrate the wood, maintaining the initial structure inside the wood. The energy-dispersive X-ray (EDX) pattern and X-ray photoelectron spectroscopy (XPS) both prove the successful doping of Fe (Figs. 6(b) and 6(c)). Figures 6(d) and 6(e) present the Ti2p and Fe2p XPS spectra of the film, respectively. According to the peak-fitting results, all titanium ions in the film have valence Ti^{4+}, and the doped Fe^{3+} combines with oxygen and exists in the composite film in the form of Fe_2O_3. Figure 6(f) shows the degradation of MO by STCF with different Fe^{3+} doping amounts after 2 h of 30 W UV lamp irradiation. When the wood is coated with Fe^{3+} -free STCF, the degradation rate reaches 19.55%. By contrast, when the doping amount of Fe^{3+} is increased to 1 wt%, the degradation rate reaches a

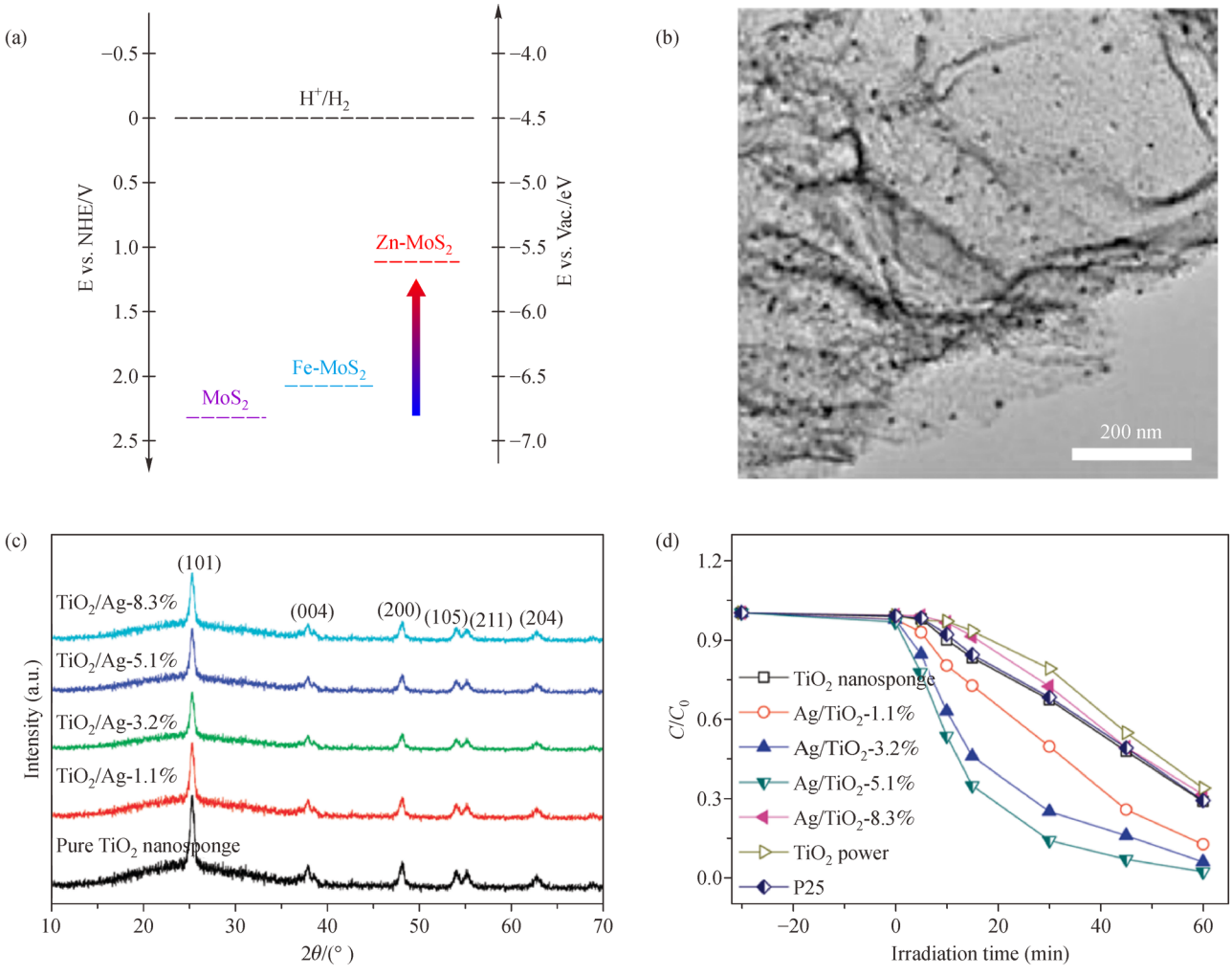

Fig. 5 Improvement of photocatalytic activity by metal element doping. (a) Mechanism diagram of element doping; (b) transmission electron microscopy (TEM) image of TiO_2/Ag; (c) XRD patterns of TiO_2/Ag and pure TiO_2 nanosponge; (d) photocatalytic degradation property before and after the doping toward aqueous salicylic acid (a. Adapted from Shi et al. (2017) with the permission of the American Chemical Society; b−d. Adapted from Yu et al. (2012) with the permission of the American Chemical Society) .

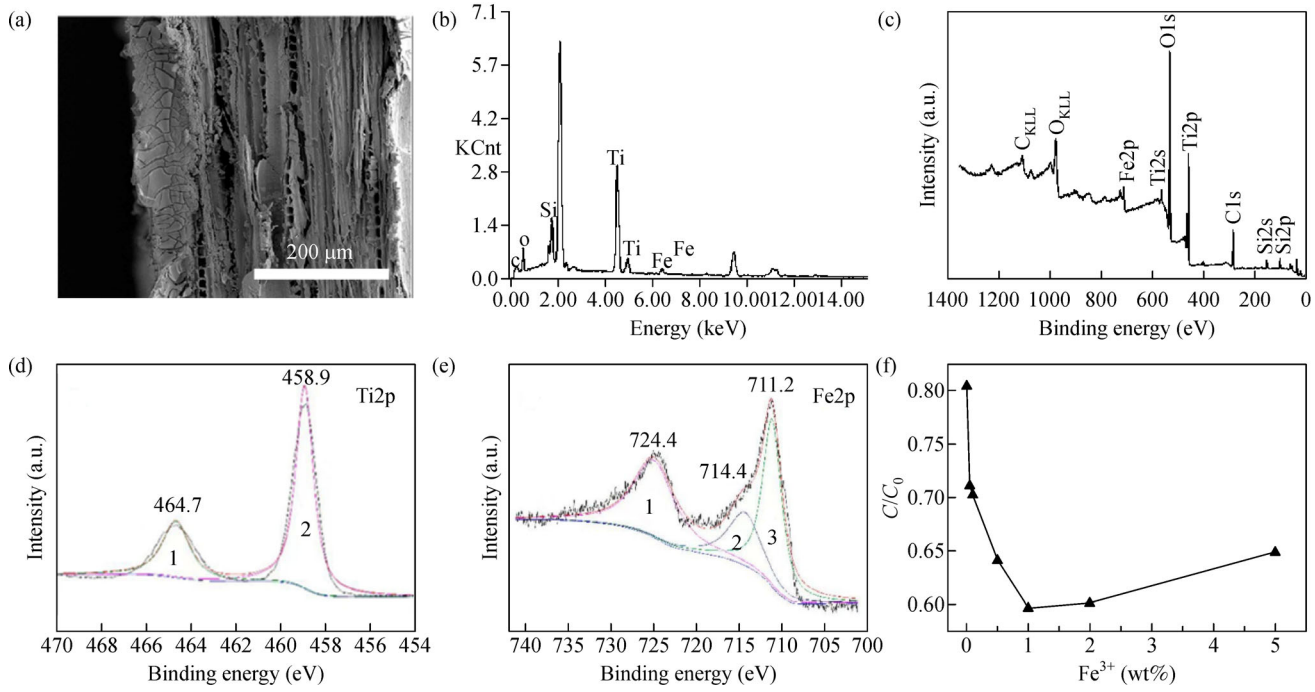

Fig. 6 Micromorphology, chemical composition and photocatalytic property of Fe^{3+}-doped STCF. (a) Joint surface between Fe^{3+}-doped STCF and wood; (b) EDX pattern and (c) XPS survey spectrum of STCF-1; (d) Ti2p and (e) Fe2p XPS spectra of Fe^{3+} -doped STCF; (f) relationship between Fe^{3+} doping content and degradation of MO (Adapted from Xuan et al. (2018) with the permission of the Multidisciplinary Digital Publishing Institute).

maximum (40.37%). However, when the doping amount of Fe^{3+} is higher than 1 wt%, the degradation rate decreases since Fe-related oxides do not have independent phases and thus doping results in smaller grain sizes.

3.2 Photocatalytic activity improved by micromorphology control

Micromorphology of photocatalytically active substances is also crucial. As a result, it is meaningful to control the microstructure of photocatalysts in the synthetic process. Taking hydrothermal synthesis as an example, it is common to adjust various reaction parameters (such as pH value (Li et al., 2019), time (Fu et al., 2019) and concentration (Zhu et al., 2016) during the hydrothermal method to acquire different photocatalyst morphologies. (Zhu and Hu, 2014) adopted a morphologically controllable supercritical hydrothermal method to prepare various TiO_2 nanostructures. Through specific crystal phase growth at different pH (i.e., 14.1, 13.2 and 12.4), the morphologies (including spherical, flake and rod) are successfully acquired (Figs. 7(a)−7(c)). For the mechanism, the oriented growth is associated with the generation of rods, and the stronger bonding interaction between atoms in the same layer leads to the formation of flakes (Fig. 7(d)). Similarly, Li et al. (2018) used a hydrothermal method to synthesize a class of wood-supported bismuth molybdate photocatalysts (W-BMO). By adjusting the pH value with NaOH aqueous solution, the micromorphology of Bi_2MoO_6 could be well controlled. When the pH value rises from 5 to 9, the crystal shape gradually changes from microspheres to cubic crystals (Fig. 8(a)).

Additionally, the degradation effect of RhB is different when using different crystals morphologies, as displayed in Fig. 8(b). Before irradiation, the degradation of RhB resulting from adsorption could reach 37% for W-BMO-6. The photodegradation efficiency of W-BMO samples is highest when the pH is 6, and the degradation of RhB is close to 99% after 60 min of irradiation. This outstanding property is because the crystal morphology formed at pH = 6 has the largest pore volume, which can provide more superficial active sites that are helpful for improving the photocatalytic activity. The optical absorption properties of the W-BMO and Bi_2MoO_6 samples were evaluated by UV-Vis diffuse reflectance spectroscopy (DRS). Figure 8c indicates that the spectra of both samples have almost the same shape. Also, in the range of visible light, the strong absorption suggests the photo-responsive activity of the composite in this light range. Besides, the absorption intensity varied with pH value.

Liu et al. (2017) employed microwave-assisted hydrothermal technology to prepare a wood cellulose/ZnO precursor, and then thermally converted it into a ZnO/carbon composite. By calcination in N_2, the cellulose became disordered carbon particles, and ZnO crystals were

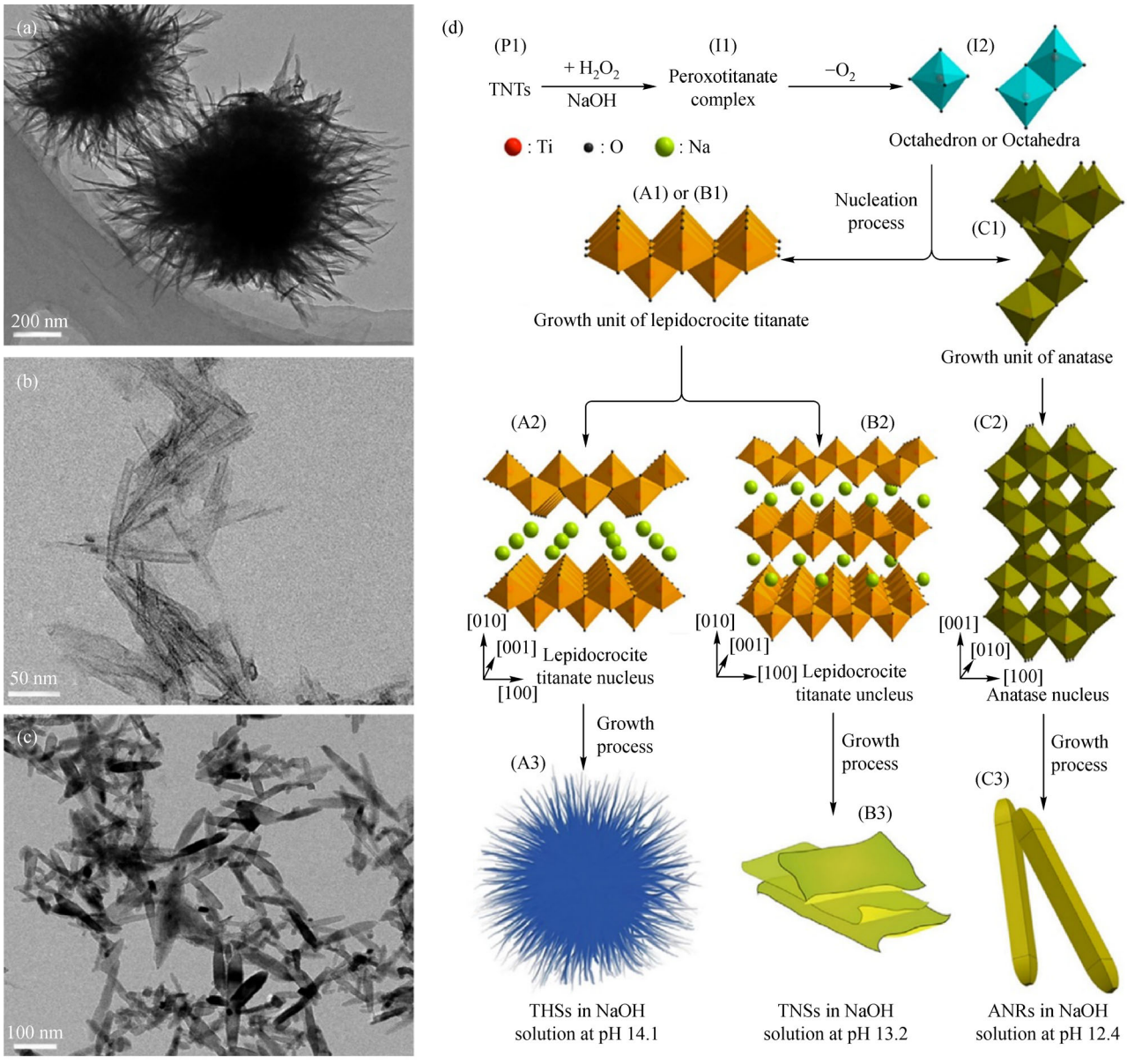

Fig. 7 Improved of photocatalytic activity of TiO_2 nanostructures by micromorphology control. (a–c) TEM images of THSs, TNSs and ANRs; (d) formation mechanisms of different TiO_2 nanostructures (Adapted from Zhu and Hu. (2018) with the permission of the Elsevier) .

tightly adhered to the carbon surface. When the concentration of Zn^{2+} is 0.02 mol/L, nanoflower-like ZnO crystals were generated. When the concentration of Zn^{2+} increases to 0.06 mol/L, a higher crystallinity was obtained. The degradation rates of methylene blue (MB) by the composite prepared with Zn^{2+} = 0.02 mol/L and Zn^{2+} = 0.06 mol/L are 74.49% and 96.67% (UV-Vis radiation, 240 min), respectively; the degradation rates of RhB are 52.93% and 55.61%, respectively. The results demonstrate that Zn^{2+} = 0.06 mol/L prefers for the acquirement of superior activity. Dang et al. (2017) adopted a convenient hot-pressing method to prepare polyethylene/nano-ZnO/wood fiber (PZW) composites. With increasing ZnO content, the surface color of the composites from PZW0 (0% ZnO) to PZW4 (8% ZnO) faded. Moreover, the surface micromorphology became rough as the ZnO content increased. PZW4 delivered the best degradation effect of MO under UV irradiation for 300 min (approximately 84%), demonstrating that the higher ZnO content achieved improved photocatalytic activity. Apart from the above methods, there are some other approaches (for instance, magnetron sputtering (Rondiya et al., 2017; Du et al., 2018) and electroless plating (Jiang et al., 2016; Venkatakrishnan and Karthik, 2019), which are also able to adjust the photocatalytic performance by controlling the micromorphology of photocatalysts.

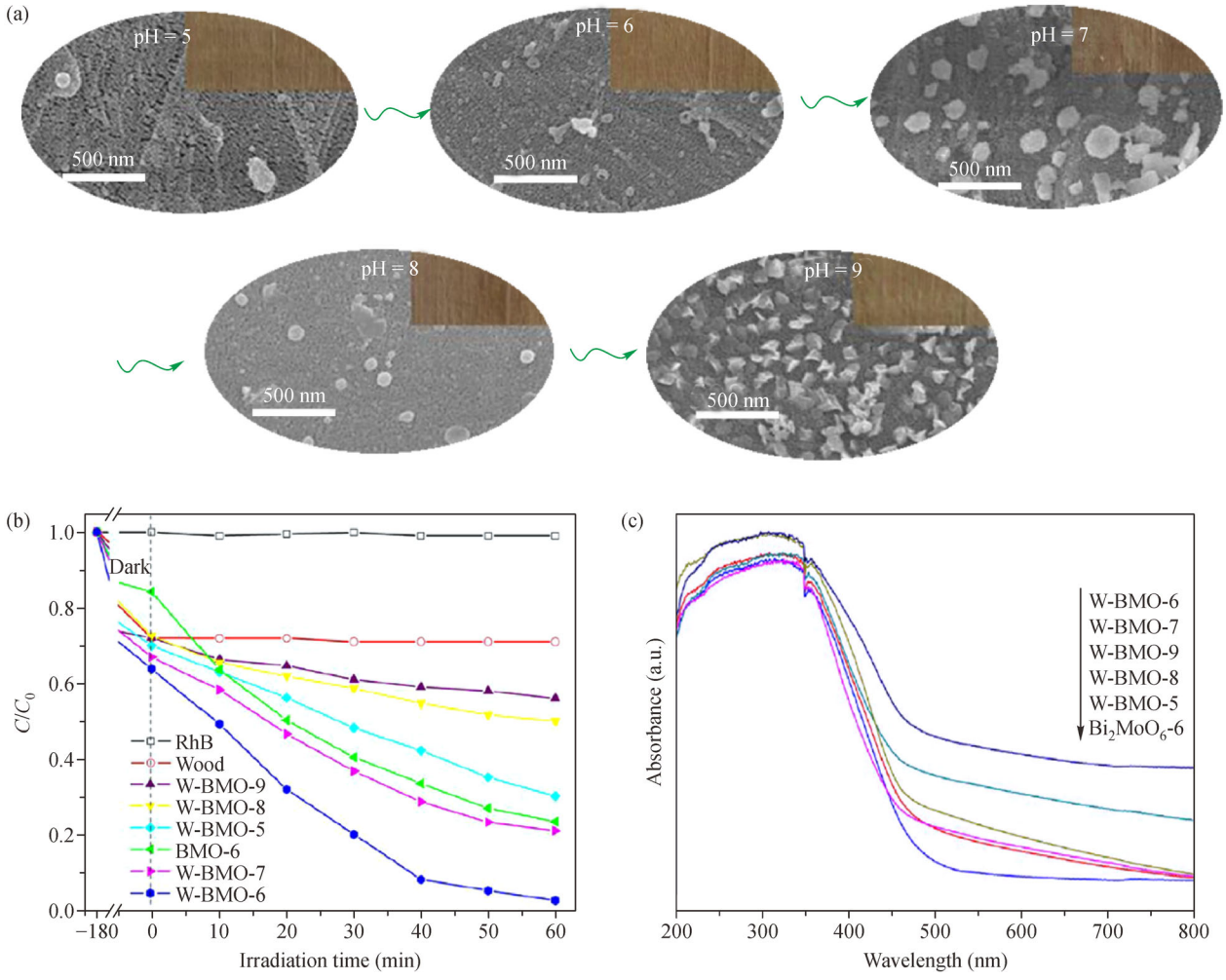

Fig. 8 Improvement of photocatalytic property of W-BMO by micromorphology control. (a) SEM images of W-BMO samples at different pH; (b) photocatalytic degradation efficiency of RhB; (c) UV-Vis DRS. (Adapted from Li et al. (2018) with the permission of the Elsevier) .

3.3 Photocatalytic activity improved by semiconductor coupling

Semiconductor coupling, namely the construction of semiconductor heterostructures, is another important pathway. More importantly, by virtue of semiconductor coupling, multiple-component photocatalysts commonly display higher photocatalytic activity and visible-light responsiveness than single-component photocatalysts. Taking the SnO_2-TiO_2 system as an example, according to study by Vinodgopal and Kamat (1995), the enhanced photocatalytic degradation rate is ascribed to the coupling of different energy levels of SnO_2 and TiO_2, resulting in the improved charge separation. Based on photoelectrochemical measurements on single and coupled semiconductor films, the SnO_2-TiO_2 coupled films achieve higher photon-to-photocurrent conversion efficiency. Similarly, TiO_2 or ZnO/CdS is also a famous coupled semiconductor system delivering improved charge separation (Ozcan et al., 2019). To date, there are many instructive studies on wood substrate-supported coupled semiconductors. For instance, Gao et al. (2017) used wood fiber as the substrate to support WO_3/TiO_2 photocatalysts by means of a combined two-step hydrothermal method and calcination (as shown in Fig. 9). The wood fiber substrate provides a high surface area; i.e., the as-prepared WO_3/TiO_2 in the presence of wood fiber achieves a BET surface area approximately 3.6 times higher than that of WO_3/TiO_2 obtained in the absence of wood fiber (Fig. 10(a)). Moreover, the presence of wood fiber induces the homogeneous growth of spherical TiO_2 and actinomorphic WO_3 flowers (Figs. 10(b) and 10(c)). Regarding the photocatalytic activity, compared to TiO_2-wood fiber, the WO_3/TiO_2-wood fiber has a faster removal ability and higher photodegradation efficiency for MO, MB and RhB (Figs. 10(d)−10(f)). However, as shown in Figs. 10(d)−10(f), the degradation ratios of RhB, MB and MO due to adsorption are below 10% because of the low porosity of

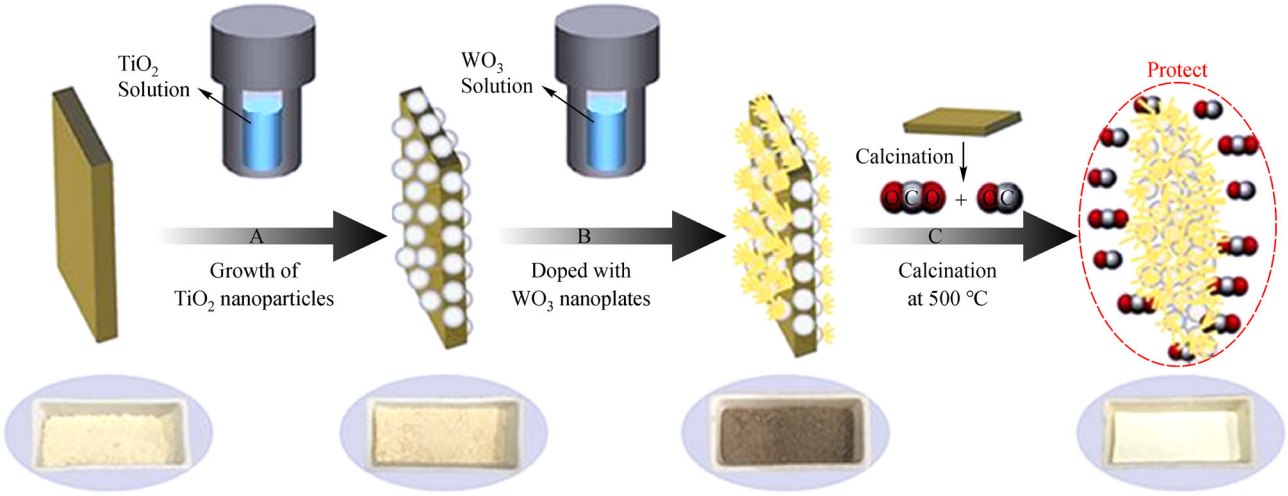

Fig. 9 Synthesis scheme of WO_3/TiO_2-wood fiber photocatalysts (Adapted from Gao et al. (2017) with the permission of the Springer Nature) .

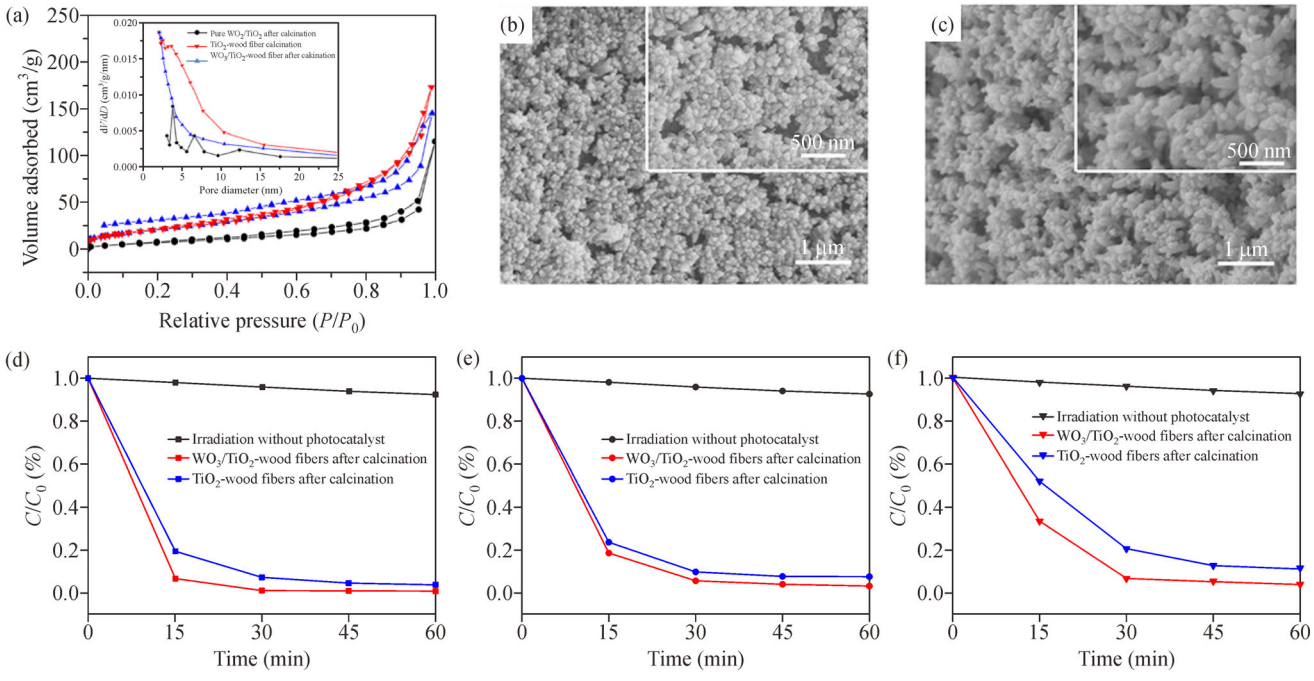

Fig. 10 Microstructure, surface area and photocatalytic activity of wood fiber-supported heterostructured WO_3/TiO_2 photocatalysts. (a) N_2 adsorption–desorption isotherms and the inset shows the pore size distributions; SEM images of (b) actinomorphic WO_3 flowers and (c) of spherical TiO_2; (d–f) the concentration percentage (C/C_0) of photocatalytic RhB (d), MB (e) and MO (f) using different photocatalysts (Adapted from Gao et al. (2017) with the permission of the Springer Nature) .

the TiO_2-wood fiber. In Fig. 11, electrons that are excited by UV- or visible-light illumination move from the CB of WO_3 to the CB of TiO_2, hence imposing restrictions on the electron–hole recombination in the VBs of the two semiconductors. In addition, these holes directly migrate to the semiconductor interface or transfer from TiO_2 to WO_3. The restriction of recombination is primarily responsible for the photo-activity enhancement.

Xu et al. (2019) chose wood cellulose fiber as the supporting material to in situ grow BiOBr nanoflakes and AgBr nanospheres by freeze-drying (see Fig. 12(a)). The TEM image indicates that these nanosubstances are adhered to the wood cellulose fiber (see Fig. 12(b)), and the high-resolution TEM (HRTEM) image proves the presence of pure BiOBr (lattice spacing of d = 0.28 nm, (102) plane) and AgBr (d = 0.33 nm, (111) plane) (Fig. 12 (c)). The wood-derived fiber/BiOBr/AgBr (WFBA) sponge cannot only effectively adsorb RhB but also

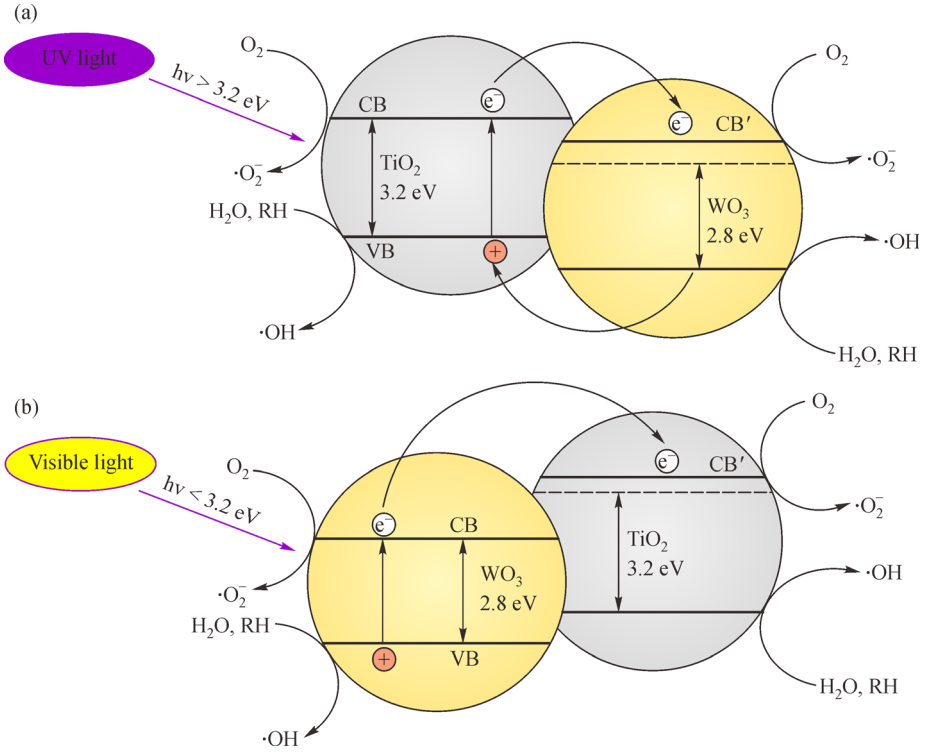

Fig. 11 Photocatalytic mechanism of the coupled WO_3/TiO_2 using wood fiber as the substrate (Adapted from Gao et al. (2017) with the permission of the Springer Nature) .

degrade it within 5 min using a Xe lamp with 15 min under solar light and within 180 min using a fluorescent lamp (Fig. 12(d)). The Fourier transform infrared spectroscopy (FTIR) bands of RhB were observed to disappear after photodegradation (Fig. 12(e)). This result reveals the almost complete degradation of RhB. The retarding of charge carries recombination and the prolonging of electron lifetime are responsible for the enhanced photocatalytic properties (Cui et al., 2013).

4 Wood reassembly-based photocatalysts for removal of organic pollutants

When directly utilizing bulk wood to prepare photocatalysts, the method is referred to a top-down process. In addition, through a top-down (namely nano-disintegration) and bottom-up (reassembly) process, the bulk wood can be transformed to various isotropic reassemblies (i.e., 1D fiber, 2D films and 3D hydrogels or aerogels) (Zhu et al., 2006; Wan et al., 2015a; Wan et al., 2018; Wan et al., 2019a; Wan et al., 2019b). More importantly, these reassemblies have higher mechanical strength, larger surface area and pore volume and more flexibility, than bulk wood. For the reassembly mechanism, the well-dispersed cellulose chains, which are disintegrated from the wood cell wall, can reconnect with each other by hydrogen-bonding interactions based on various methods (like solvent evaporation and the addition of anti-solvent), eventually leading to the formation of wood reassemblies (Fig. 13(a)).

Table 1 summarizes recent progress on wood reassembly-based photocatalysts. For instance, Wan et al. (2017) deposited TiO_2 microspheres on cellulose-based carbon fiber (denoted as CCF/TMS) via a sol-gel and pyrolysis and studied the photocatalytic activity of the composites toward indigo carmine, when using CCF/TMS composites, the dark blue dye solution quickly turned colorless within 40 min. Additionally, a faster decomposition rate of indigo carmine dye was achieved in the case of CCF/TMS than with TiO_2 P25 and anatase TiO_2. Xiao et al. (2018) created carbon/ZnO hybrids using TEMPO-oxidized cellulose as a reactive template by virtue of a low-temperature precipitation method. The composites show a significant MO photodegradation of 96.11% within 120 min. Ghoreishian et al. (2016) deposited ZnO@TiO_2 photocatalysts onto 3D spacer fabrics by magnetron sputtering. The photocatalysts can fastly decolorize textile effluent. Bai et al. (2020) prepared porous g-C_3N_4/cellulose photocatalysts through co-assembling g-C_3N_4 and cellulose. Thanks to the synergistic effect of adsorption and photocatalysis, approx. 99.8% degradation rate of MB is achieved (Fig. 13(b)), as compared to that of pure g-C_3N_4 (54.2%). The good interface facilitates the transfer of photogenerated electrons (Fig. 13(c)).

In addition to excellent photocatalytic properties, the recovery and reuse function in a continuous degradation cycle is important for photocatalysts. Easy post-treatment

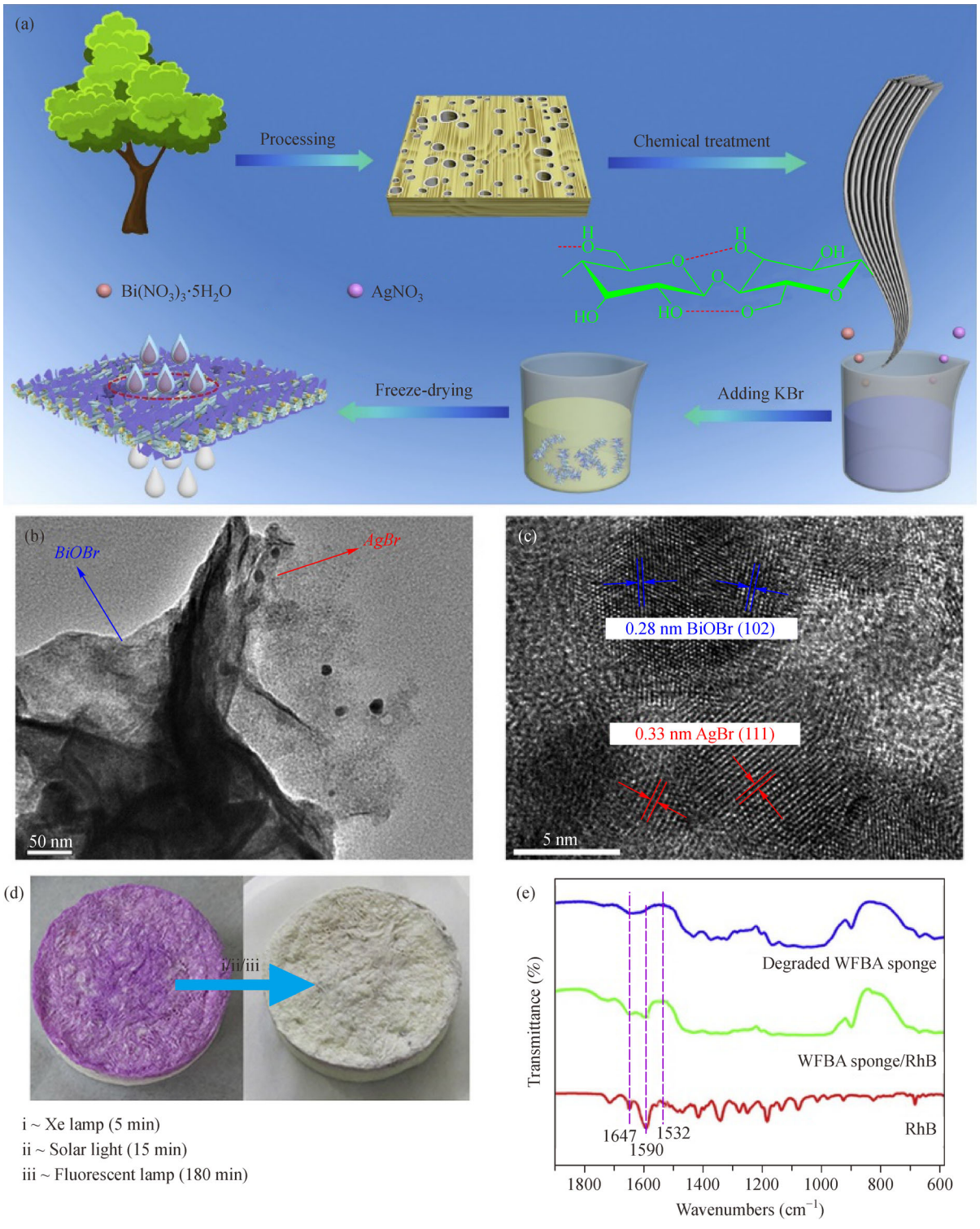

Fig. 12 Preparation strategy, microstructure, and photocatalytic activity of WFBA sponge. (a) Fabrication of WFBA sponge; (b) TEM image of the WFBA; (c) HRTEM image of WFBA indicating the lattice spacings of BiOBr and AgBr; (d) photographs and (e) FTIR spectra before and after RhB degradation (Adapted from Xu et al. (2019) with the permission of the Elsevier) .

and efficient reuse can greatly improve the service life of photocatalysts. Morshed et al. (2020) prepared novel cellulose nanowhisker-supported TiO_2 (CN@nTiO_2) photocatalysts via a low-temperature sol-gel method. The reusability of CN@nTiO_2 for the photocatalytic degradation of MB was studied. As shown in Fig. 14a and b, after each cycle, the catalyst was recovered by simple filtration and then used in the next cycle. The results indicated that

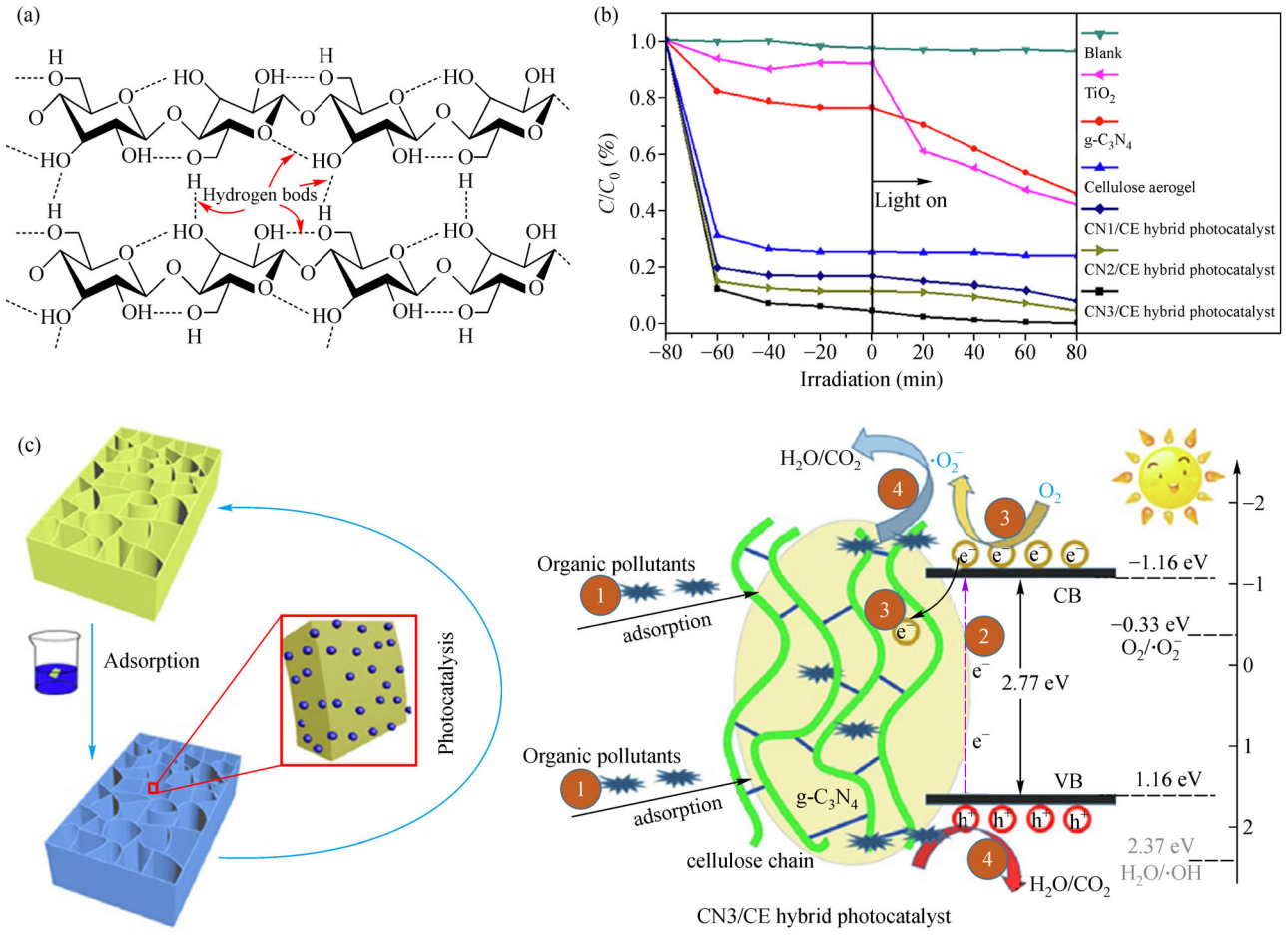

Fig. 13 Removal ability of g-C_3N_4/cellulose hybrid photocatalyst for MB. (a) Schematic diagram of the repeating unit of cellulose chain; (b) Contributions of adsorption and photocatalysis under visible-light irradiation of different samples for MB degradation; (c) schematic illustration of g-C_3N_4/cellulose hybrid photocatalyst for MB degradation (a. Adapted from Wan et al. (2019b) with the permission of the Elsevier; b. Adapted from Bai et al. (2020) with the permission of the Elsevier) .

the as-prepared photocatalyst could be reused more than five times with each test providing a conversion efficiency of up to 80%. The reason for these results is that there are many Ti atoms in CN@nTiO_2 and the crucial role of metal-organic electrostatic attraction makes it a favorable recyclable photocatalyst. Interestingly, Nasiri et al. (2019) adopted a microwave-assisted method to obtain a magnetically separable photocatalyst (i.e., $CoFe_2O_4$@-methylcellulose). The saturation magnetization is 40.05 emu/g (see Fig. 14(c)). The photocatalytic activity of the nano-$CoFe_2O_4$@MC photocatalyst decreased significantly in the second use, but remained stable from the second run to the fourth run. The degradation rate was 77.58% for the fourth run (Fig. 14(d)). This performance is observed because there are many Fe and Co metal ions and a high surface area in $CoFe_2O_4$@MC, ensuring insignificant loss of photocatalytic activity from the second run to the fourth run.

Thomas et al. (2016) used dissipative convection and freeze-drying to successfully obtain TiO_2-NP-encapsulated Ba-ion crosslinked alginate/carboxymethyl cellulose (CMC) nanocomposite hydrogels. The catalysts exhibited good adsorption and degradation performance. Figure 14 (e) shows that during the adsorption process, 40% of the Congo red (CR) dye was adsorbed within 30 min. After that point, the removal rate of dye due to adsorption was quite slight. For the synergistic effects of adsorption and photocatalysis, through 240 min of exposure to sunlight, a degradation rate of 91.5% was obtained. Besides, cyclability is one criterion for measuring the stability of photocatalysts. In Fig. 14(f), the composite has a stable photocatalytic activity for the succedent four cycles, which is attributed to the synergy of Ba/Alg/CMC and TiO_2. Furthermore, this composite gel is nontoxic, economically feasible, and harmless to the environment.

Li et al. (2017) electrospun a composite nanofiber membrane which is composed of cellulose acetate (CA) and $H_4SiW_{12}O_{40}$ (SiW_{12}). The photocatalytic property of the electrospun composite membrane toward tetracycline (TC) and MO is superior to that of pure SiW_{12}, and

achieves the maximum at $m_{SiW_{12}} : m_{CA} = 1 : 4$ (Fig. 14 (g)). The composite film also exhibited satisfactory reusability. As presented in Figs. 14(h) and 15(i), the degradation efficiency of MO and TC in the third cycle is 75.6% and 49.4%, respectively, which is attributed to the hydrogen-bonding interactions between them.

5 Conclusions and outlook

Significant progress in the development of wood and wood-derivative-based catalysts for the photodecomposition of organic pollutants in water environment has been achieved in the past few years, owing to their environmental friendliness, exceptional structures and properties. In the current review, the recent advances in this area have been summarized, mainly focusing on the hierarchical structure and features of wood, strategies of designing novel photocatalysts using wood or its recombinants, and effective methods (including metal element doping, morphology control and semiconductor coupling) for improving the photocatalytic activity. Owing to the efforts of many researchers, a rich variety of wood-derived photocatalysts have been created via various fabrication methods (Table 1). Unquestionably, the development of green, high-performance, and recyclable wood-derived photocatalysts will still be a significant focus in future research.

Although wood or its recombinants (such as 1D fiber, 2D films and 3D porous gels) have been successfully used

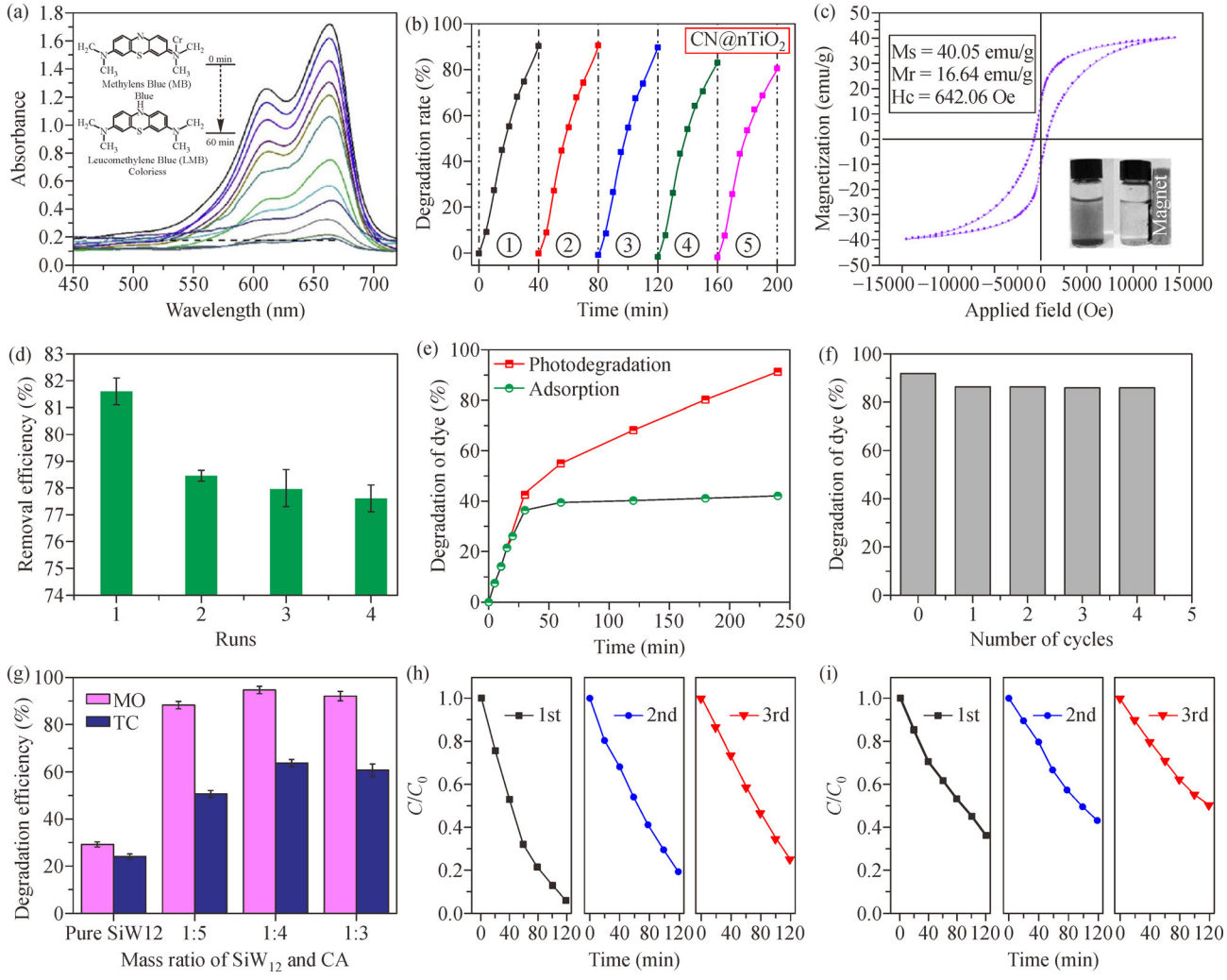

Fig. 14 Recyclability of CN@nTiO$_2$, CoFe$_2$O$_4$@MC, Ba/Alg/CMC/TiO$_2$ and SiW$_{12}$/CA. (a) UV-Vis spectroscopic analysis of the photocatalytic decoloration of MB; (b) recyclability of CN@nTiO$_2$; (c) magnetization curve of CoFe$_2$O$_4$@MC with the inset showing the magnetic separation phenomenon; (d) recycling and reuse of nanoCoFe$_2$O$_4$@MC for MNZ degradation; (e) photodegradation and adsorption and (f) cyclicity of Ba/Alg/CMC/TiO$_2$ on CR; (g) effect of mass ratios of SiW$_{12}$ and CA on degradation efficiency of MO and TC; (h–i) recyclability of SiW$_{12}$/CA for (h) MO and (i) TC. (a–b. Adapted from Morshed et al. (2020) with the permission of the Elsevier; c–d. Adapted from Nasiri et al. (2019) with the permission of the Springer; e-f. Adapted from Thomas et al. (2016) with the permission of the Elsevier; g–i. Adapted from Li et al. (2017) with the permission of the Elsevier) .

Table 1 Preparation method, micromorphology, and their photocatalytic activity of recently reported wood or its reassemblies-based photocatalysts.

Wood-derived photocatalysts	Preparation methods	Pollutants	Morphology	Maximum activity	Ref.
TiO_2/cellulose aerogels	Hydrothermal	RhB & MO	3D network	RhB: ~99% 1 h MO: ~100% 1 h	Wan et al. (2015b)
ZnO/cellulose acetate-polyurethane membrane	Solution dispersion blending	RR[a] 11 & RO[b] 84	2D sheets	RR 11 ~95% 0.67 h RO 84 ~90% 0.67 h	Rajeswari et al.(2017)
TiO_2/Ag/cellulose nanosponge	Sol-gel	Salicylic acid	3D sponge	~97.8% 1 h	Yu et al. (2012)
Fe^{3+}-doped STCF	Sol-gel	MO	2D sheets	~40.37% 2 h	Xuan et al. (2018)
W-BMO	Hydrothermal	RhB	Microspheres/cube	~99% 1 h	Li et al.(2018)
Cellulose/ZnO	Hydrothermal	RhB & MB	Flower/particles	RhB ~55.6% 4 h MB ~96.67% 4 h	Liu et al. (2017)
PZW	Hot-pressing	MO	2D sheets/particles	~84% 5 h	Dang et al. (2017)
WO_3/TiO_2-wood fiber	Hydrothermal method and calcination	MO, MB & RhB	Spheres/flowers	MO ~96.6% 0.75 h MB ~96.6% 0.75 h RhB ~99.8% 0.75 h	Gao et al. (2017)
Wood-derived fiber/BiOBr/AgBr	Freeze-drying	RhB	Nanosheets/nanospheres	~99.90% 5 min	Xu et al. (2019)
CCF/TMS	Immersion-drying-pyrolysis	Indigo carmine	Filiform/spherical particles	~90% 0.67 h	Wan et al. (2017)
Carbon/ZnO	Chemical precipitation	MO	Rod	~96.11% 2 h	Xiao et al. (2018)
ZnO@TiO_2/3D spacer fabrics	Magnetron sputtering	Azo	Network/particles	~100% 1 h	Ghoreishian et al.(2016)
g-C_3N_4/cellulose aerogels	Co-assembly	MB	Network	~99.8% 1.33 h	Bai et al. (2020)
CN@nTiO_2	Sol-gel	MB	Core-shell	~90% 0.67 h	Morshed et al. (2020)
$CoFe_2O_4$@methlycellulose	Microwave-assisted	MNZ[c]	Sphere-shaped particles	~85.30% 2 h	Nasiri et al. (2019)
Cellulose/TiO_2 hydrogel	Dissipative convective	CR	3D network	~91.5% 4h	Thomas et al. (2016)
$H_4SiW_{12}O_{40}$ (SiW_{12})/cellulose acetate (CA) membrane	Electrospinning	TC & MO	2D sheets	TC ~65% 2h MO ~95% 2h	Li et al.(2017)

Note:[a]RR: reactive red; [b]RO: reactive orange; [c]MNZ: metronidazole.

to create a series of advanced photocatalysts for the degradation of organic pollutants, there are still some issues needing to be solved.

1) Novel wood-derived substrates. The porosity of substates and their surface group content critically affect the loading and uniformity of nanomaterials, which are key for the photocatalytic activity, adsorption capacity and recoverability of wood-derived photocatalysts. Therefore, it is quite senseful to create new strategies to tun the pore structure (like pore size and porosity) of wood-based substrates. In addition, attention needs to be paid to the mechanical strength. Also, necessary modification treatments (for instance, grafting, copolymerization, and carboxylation) are beneficial for the stability of nanomaterials on the substrate surfaces.

2) New pathways to strengthen the activity. The visible-light photocatalytic activity plays a decisive role in the use and popularization of photocatalysts. In addition to the three typical methods listed (namely the metal element doping, morphology control and semiconductor coupling), other methods (such as introducing oxygen defects and performing surface sensitization) are also useful to improve the photocatalytic activity of wood-derived photocatalysts, by reducing the band gap of semiconductors and slowing electron–hole recombination.

3) Large-scale manufacturing. Although the synthesis of photocatalysts has matured over the past decade, the fabrication of wood-derived photocatalysts is still at the laboratory scale. It is difficult to perform large-scale production of wood-derived photocatalysts with high uniformity. We should pay more attention to developing new methods and equipment to simplify the synthesis

process of wood-based substrates and the subsequent integration process with nanomaterials. More importantly, the involved costs should be reduced to a minimum a level as possible.

Acknowledgements This study was supported by the National Natural Science Foundation of China (Grant Nos. 31901249 and 31890771), the Young Elite Scientists Sponsorship Program by CAST (Grant No. 2019QNRC001), the Scientific Research Foundation of Hunan Provincial Education Department (Grant No. 18B180), the China Postdoctoral Science Foundation (Grant No. 2020M672846) and the Outstanding Chinese and Foreign Youth Exchange Program of China Association of Science and Technology.

References

Akpan U, Hameed B (2010). The advancements in sol-gel method of doped-TiO_2 photocatalysts. Applied Catalysis A, General, 375(1): 1–11

Bai S, Jiang J, Zhang Q, Xiong Y J (2015). Steering charge kinetics in photocatalysis: intersection of materials syntheses, characterization techniques and theoretical simulations. Chemical Society Reviews, 44(10): 2893–2939

Bai W, Yang X, Du X, Qian Z, Zhang Y, Liu L, Yao J (2020). Robust and recyclable macroscopic g-C_3N_4/cellulose hybrid photocatalysts with enhanced visible light photocatalytic activity. Applied Surface Science, 504: 144179

Byun J, Zhang K A (2020). Designing conjugated porous polymers for visible light-driven photocatalytic chemical transformations. Materials Horizons, 7(1): 15–31

Carey J H, Lawrence J, Tosine H M (1976). Photodechlorination of PCB's in the presence of titanium dioxide in aqueous suspensions. Bulletin of Environmental Contamination and Toxicology, 16(6): 697–701

Chong M N, Jin B, Chow C W, Saint C (2010). Recent developments in photocatalytic water treatment technology: A review. Water Research, 44(10): 2997–3027

Cojocaru B, Neaţu Ş, Sacaliuc-Pârvulescu E, Lévy F, Pârvulescu V I, Garcia H (2011). Influence of gold particle size on the photocatalytic activity for acetone oxidation of Au/TiO_2 catalysts prepared by dc-magnetron sputtering. Applied Catalysis B: Environmental, 107(1–2): 140–149

Cui W, Ma S, Liu L, Hu J, Liang Y, Mcevoy J G (2013). Photocatalytic activity of Cd1-$x$$Zn_xS$/$K_2Ti_4O_9$ for rhodamine B degradation under visible light irradiation. Applied Surface Science, 271: 171–181

Dang B, Chen Y, Shen X, Chen B, Sun Q, Jin C (2017). Fabrication of a nano-ZnO/polyethylene/wood-fiber composite with enhanced microwave absorption and photocatalytic activity via a facile hot-press method. Materials (Basel), 10(11): 1267

Devi L G, Kavitha R (2013). A review on non-metal ion doped titania for the photocatalytic degradation of organic pollutants under UV/solar light: Role of photogenerated charge carrier dynamics in enhancing the activity. Applied Catalysis B: Environmental, 140-141: 559–587

Du L, Wong H, Dong S, Lau W S, Filip V (2018). AFM study on the surface morphologies of TiN films prepared by magnetron sputtering and Al_2O_3 films prepared by atomic layer deposition. Vacuum, 153: 139–144

Ebrahimzadeh M A, Mortazaviderazkola S, Zazouli M A (2020a). Eco-friendly green synthesis of novel magnetic Fe_3O_4/SiO_2/ZnO-Pr_6O_{11} nanocomposites for photocatalytic degradation of organic pollutant. Journal of Rare Earths, 38(1): 13–20

Ebrahimzadeh M A, Naghizadeh A, Amiri O, Shirzadi-Ahodashti M, Mortazavi-Derazkola S (2020b). Green and facile synthesis of Ag nanoparticles using crataegus pentagyna fruit extract (CP-AgNPs) for organic pollution dyes degradation and antibacterial application. Bioorganic Chemistry, 94: 103425

Fan L, Liu Z, Zhu Y, Wang Z, Zhao S, Zhu L, Zhang Q (2020). Synthesis of Li-doping tetragonal-Bi_2O_3 nanomaterial with high efficient visible light photocatalysis. Journal of Materials Science Materials in Electronics, 31(3): 2100–2110

Fu X, Huo W, Liu X, Shan Q, Guo Z, Jing C, Dong F, Yao H C, Zhang Y, Chen K (2019).Morphological evolution process of δ-MnO2 from 2-D to 1-D without phase transition . Crystengcomm, 21(31): 4593–4598

Fujishima A, Honda K (1972). Electrochemical photolysis of water at a semiconductor electrode. Nature, 238(5358): 37–38

Fujiwara T, Sasahara A, Happo N, Kimura K, Hayashi K, Onishi H (2020). Single-crystal model of highly efficient water-splitting photocatalysts: A $KTaO_3$ wafer doped with calcium cations. Chemistry of Materials, 32(4): 1439–1447

Gao G, Jiao Y, Waclawik E R, Du A (2016). Single atom (Pd/Pt) supported on graphitic carbon nitride as an efficient photocatalyst for visible-light reduction of carbon dioxide. Journal of the American Chemical Society, 138(19): 6292–6297

Gao L, Gan W, Qiu Z, Zhan X, Qiang T, Li J (2017). Preparation of heterostructured WO_3/TiO_2 catalysts from wood fiber and its versatile photodegradation abilities. Scientific Reports, 7(1): 1102

Gao L, Li S, Huang D, Shen Y, Wang M (2015). ZnO decorated TiO_2 nanosheet composites for lithium ion battery. Electrochimica Acta, 182: 529–536

Gautam S, Shandilya P, Priya B, Singh V P, Raizada P, Rai R, Valente M, Singh P (2017). Superparamagnetic $MnFe_2O_4$ dispersed over graphitic carbon sand composite and bentonite as magnetically recoverable photocatalyst for antibiotic mineralization. Separation and Purification Technology, 172: 498–511

Gezimati J, Singh H, Creamer L K (1996). Heat-induced interactions and gelation of mixtures of bovine β-lactoglobulin and serum albumin. Journal of Agricultural and Food Chemistry, 44(3): 804–810

Ghoreishian S M, Badii K, Norouzi M, Malek K (2016). Effect of cold plasma pre-treatment on photocatalytic activity of 3D fabric loaded with nano-photocatalysts: Response surface methodology. Applied Surface Science, 365(3): 252–262

Giri S, Singh A K (2014). Assessment of surface water quality using heavy metal pollution index in Subarnarekha River, India. Water Quality, Exposure, and Health, 5(4): 173–182

Gu J, Yu H, Quan X, Chen S, Niu J (2020). Utilizing transparent and conductive SnO_2 as electron mediator to enhance the photocatalytic performance of Z-scheme Si-SnO_2-TiOx. Frontiers of Environmental Science & Engineering, 14(4):72

Guo Q, Zhou C, Ma Z, Yang X (2019). Fundamentals of TiO_2 photocatalysis: Concepts, mechanisms, and challenges. Advanced Materials, 31(50): 1901997

Gusain R, Kumar N, Ray S S (2020). Recent advances in carbon

nanomaterial-based adsorbents for water purification. Coordination Chemistry Reviews, 405: 213111

Han Q, Hu C, Zhao F, Zhang Z, Chen N, Qu L (2015). One-step preparation of iodine-doped graphitic carbon nitride nanosheets as efficient photocatalysts for visible light water splitting. Journal of Materials Chemistry. A, Materials for Energy and Sustainability, 3 (8): 4612–4619

Hao X, Wang G, Chen S, Yu H, Quan X (2019). Enhanced activation of peroxymonosulfate by CNT-TiO_2 under UV-light assistance for efficient degradation of organic pollutants. Frontiers of Environmental Science & Engineering, 13(5):77

Heo C H, Lee S B, Boo J H (2005). Deposition of TiO_2 thin films using RF magnetron sputtering method and study of their surface characteristics. Thin Solid Films, 475(1–2): 183–188

Hong R Y, Pan T, Qian J, Li H (2006). Synthesis and surface modification of ZnO nanoparticles. Chemical Engineering Journal, 119(2): 71–81

Hu Z, Xu T, Fang B (2017). Photocatalytic degradation of vehicle exhaust using Fe-doped TiO_2 loaded on activated carbon. Applied Surface Science, 420: 34–42

Huang J, Matsumura T, Yu G, Deng S, Yamauchi M, Yamazaki N, Weber R (2011). Determination of PCBs, PCDDs and PCDFs in insulating oil samples from stored Chinese electrical capacitors by HRGC/HRMS. Chemosphere, 85(2): 239–246

Huang M, Xu C, Wu Z, Huang Y, Lin J, Wu J (2008). Photocatalytic discolorization of methyl orange solution by Pt modified TiO_2 loaded on natural zeolite. Dyes and Pigments, 77(2): 327–334

Ide Y, Inami N, Hattori H, Saito K, Sohmiya M, Tsunoji N, Komaguchi K, Sano T, Bando Y, Golberg D, Sugahara Y (2016). Remarkable charge separation and photocatalytic efficiency enhancement through interconnection of TiO_2 nanoparticles by hydrothermal treatment. Angewandte Chemie International Edition, 55(11): 3600–3605

Iguchi Y, Ichiura H, Kitaoka T, Tanaka H (2003). Preparation and characteristics of high performance paper containing titanium dioxide photocatalyst supported on inorganic fiber matrix. Chemosphere, 53 (10): 1193–1199

Janbandhu S, Joshi A, Munishwar S, Gedam R (2019). CdS/TiO_2 heterojunction in glass matrix: synthesis, characterization, and application as an improved photocatalyst. Applied Surface Science, 497: 143758

Jiang B, Yang X, Niu W, He C, Shi C, Zhao N (2016). Ultralight Co/Ag composite foams: synthesis, morphology and compressive property. Scripta Materialia, 117: 68–72

Jiang G, Lin Z, Chen C, Zhu L, Chang Q, Wang N, Wei W, Tang H (2011). TiO_2 nanoparticles assembled on graphene oxide nanosheets with high photocatalytic activity for removal of pollutants. Carbon, 49(8): 2693–2701

Jin Z, Hu R, Wang H, Hu J, Ren T (2019). One-step impregnation method to prepare direct Z-scheme $LaCoO_3$/g-C_3N_4 heterojunction photocatalysts for phenol degradation under visible light. Applied Surface Science, 491: 432–442

Kamata R, Shiraishi F, Takahashi S, Shimizu A, Shiraishi H (2010). Reevaluation of the developmental toxicity of dieldrin by the use of fertilized Japanese quail eggs. Comparative Biochemistry and Physiology. Toxicology & Pharmacology : CBP, 152(1): 84–90

Ke D, Liu S, Dai K, Zhou J, Zhang L, Peng T (2009). CdS/regenerated cellulose nanocomposite films for highly efficient photocatalytic H_2 production under visible light irradiation. Journal of Physical Chemistry C, 113(36): 16021–16026

Kemell M, Pore V, Ritala M, Leskelä M, Lindén M (2005). Atomic layer deposition in nanometer-level replication of cellulosic substances and preparation of photocatalytic TiO_2/cellulose composites. Journal of the American Chemical Society, 127(41): 14178–14179

Khojasteh H, Safajou H, Mortazaviderazkola S, Salavatiniasari M, Heydaryan K, Yazdani M (2019). Economic procedure for facile and eco-friendly reduction of graphene oxide by plant extracts; a comparison and property investigation. Journal of Cleaner Production, 229: 1139–1147

Khojasteh H, Salavatiniasari M, Mortazaviderazkola S (2016). Synthesis, characterization and photocatalytic properties of nickel-doped TiO_2 and nickel titanate nanoparticles. Journal of Materials Science Materials in Electronics, 27(4): 3599–3607

Kuang Y, Chen C, Chen G, Pei Y, Pastel G, Jia C, Song J, Mi R, Yang B, Das S, Hu L (2019). Bioinspired solar-heated carbon absorbent for efficient cleanup of highly viscous crude oil. Advanced Functional Materials, 29(16): 1900162

Li J, Xu D (2010). Tetragonal faceted-nanorods of anatase TiO_2 single crystals with a large percentage of active {100} facets. Chemical Communications, 46(13): 2301–2303

Li J, Yu H, Sun Q, Liu Y, Cui Y, Lu Y (2010). Growth of TiO_2 coating on wood surface using controlled hydrothermal method at low temperatures. Applied Surface Science, 256(16): 5046–5050

Li N, Chang T, Gao H, Gao X, Ge L (2019). Morphology-controlled $WO^3{-}_x$ homojunction: hydrothermal synthesis, adsorption properties, and visible-light-driven photocatalytic and chromic properties. Nanotechnology, 30(41): 415601

Li W, Li T, Li G, An L, Li F, Zhang Z (2017). Electrospun $H_4SiW_{12}O_{40}$/cellulose acetate composite nanofibrous membrane for photocatalytic degradation of tetracycline and methyl orange with different mechanism. Carbohydrate Polymers, 168: 153–162

Li Y, Hui B, Gao L, Li F, Li J (2018). Facile one-pot synthesis of wood based bismuth molybdate nano-eggshells with efficient visible-light photocatalytic activity. Colloids and Surfaces. A, Physicochemical and Engineering Aspects, 556: 284–290

Li Z, Cong S, Xu Y (2014). Brookite vs anatase TiO_2 in the photocatalytic activity for organic degradation in water. ACS Catalysis, 4(9): 3273–3280

Linsebigler A L, Lu G, Yates J T Jr (1995). Photocatalysis on TiO_2 surfaces: principles, mechanisms, and selected results. Chemical Reviews, 95(3): 735–758

Liu S, Yao K, Wang B, Ma M G (2017). Microwave-assisted hydrothermal synthesis of cellulose/ZnO composites and its thermal transformation to ZnO/carbon composites. Iranian Polymer Journal, 26(9): 681–691

Liu T, Li B, Hao Y, Han F, Zhang L, Hu L (2015). A general method to diverse silver/mesoporous-metal-oxide nanocomposites with plasmon-enhanced photocatalytic activity. Applied Catalysis B: Environmental, 165: 378–388

Lu F, Astruc D (2020). Nanocatalysts and other nanomaterials for water remediation from organic pollutants. Coordination Chemistry Reviews, 408: 213180

Macwan D, Dave P N, Chaturvedi S (2011). A review on nano-TiO_2 sol-

gel type syntheses and its applications. Journal of Materials Science, 46(11): 3669–3686

Meng F, Hou N, Jin Z, Sun B, Guo Z, Kong L, Xiao X, Wu H, Li M, Liu J (2015). Ag-decorated ultra-thin porous single-crystalline ZnO nanosheets prepared by sunlight induced solvent reduction and their highly sensitive detection of ethanol. Sensors and Actuators. B, Chemical, 209: 975–982

Meng N, Ren J, Liu Y, Huang Y, Petit T, Zhang B (2018). Engineering oxygen-containing and amino groups into two-dimensional atomically-thin porous polymeric carbon nitrogen for enhanced photocatalytic hydrogen production. Energy & Environmental Science, 11 (3): 566–571

Moon R J, Martini A, Nairn J, Simonsen J, Youngblood J (2011). Cellulose nanomaterials review: Structure, properties and nanocomposites. Chemical Society Reviews, 40(7): 3941–3994

Morshed M N, Al Azad S, Deb H, Shaun B B, Shen X L (2020). Titania-loaded cellulose-based functional hybrid nanomaterial for photocatalytic degradation of toxic aromatic dye in water. Journal of Water Process Engineering, 33: 101062

Moustakas N, Katsaros F, Kontos A, Romanos G E, Dionysiou D, Falaras P (2014). Visible light active TiO_2 photocatalytic filtration membranes with improved permeability and low energy consumption. Catalysis Today, 224: 56–69

Nasiri A, Tamaddon F, Mosslemin M H, Gharaghani M A, Asadipour A (2019). New magnetic nanobiocomposite $CoFe_2O_4$@methycellulose: facile synthesis, characterization, and photocatalytic degradation of metronidazole. Journal of Materials Science Materials in Electronics, 30(9): 8595–8610

Osibanjo O, Daso A P, Gbadebo A M (2011). The impact of industries on surface water quality of River Ona and River Alaro in Oluyole industrial estate, Ibadan, Nigeria. African Journal of Biotechnology, 10(4): 696–702

Ozcan C, Turkay D, Yerci S (2019). Optical and electrical design guidelines for ZnO/CdS nanorod-based CdTe solar cells. Optics Express, 27(8): A339–A351

Palanisamy B, Babu C, Sundaravel B, Anandan S, Murugesan V (2013). Sol-gel synthesis of mesoporous mixed Fe_2O_3/TiO_2 photocatalyst: Application for degradation of 4-chlorophenol. Journal of Hazardous Materials, 252– 253: 233–242

Paramasivam I, Jha H, Liu N, Schmuki P (2012). A review of photocatalysis using self-organized TiO_2 nanotubes and other ordered oxide nanostructures. Small, 8(20): 3073–3103

Rajeswari A, Vismaiya S, Pius A (2017). Preparation, characterization of nano ZnO-blended cellulose acetate-polyurethane membrane for photocatalytic degradation of dyes from water. Chemical Engineering Journal, 313: 928–937

Ratha S, Rout C S (2013). Supercapacitor electrodes based on layered tungsten disulfide-reduced graphene oxide hybrids synthesized by a facile hydrothermal method. ACS Applied Materials & Interfaces, 5 (21): 11427–11433

Ren X, Zeng G, Tang L, Wang J, Wan J, Wang J, Deng Y, Liu Y, Peng B (2018). The potential impact on the biodegradation of organic pollutants from composting technology for soil remediation. Waste Management (New York, N.Y.), 72: 138–149

Rondiya S, Rokade A, Funde A, Kartha M, Pathan H, Jadkar S (2017). Synthesis of CdS thin films at room temperature by RF-magnetron sputtering and study of its structural, electrical, optical and morphology properties. Thin Solid Films, 631: 41–49

Safari-Amiri M, Mortazaviderazkola S, Salavatiniasari M, Ghoreishi S M (2017). Synthesis and characterization of Dy_2O_3 nanostructures: Enhanced photocatalytic degradation of rhodamine B under UV irradiation. Journal of Materials Science Materials in Electronics, 28 (9): 6467–6474

Sathishkumar P, Sweena R, Wu J J, Anandan S (2011). Synthesis of CuO-ZnO nanophotocatalyst for visible light assisted degradation of a textile dye in aqueous solution. Chemical Engineering Journal, 171 (1): 136–140

Shi Y, Zhou Y, Yang D R, Xu W X, Wang C, Wang F B, Xu J J, Xia X H, Chen H Y (2017). Energy level engineering of MoS_2 by transition-metal doping for accelerating hydrogen evolution reaction. Journal of the American Chemical Society, 139(43): 15479–15485

Shirzadiahodashti M, Ebrahimzadeh M A, Amiri O, Naghizadeh A, Mortazaviderazkola S (2020). Novel NiFe/Si/Au magnetic nanocatalyst: Biogenic synthesis, efficient and reusable catalyst with enhanced visible light photocatalytic degradation and antibacterial activity. Applied Organometallic Chemistry, 34(4): e5467

Singh J, Khan S A, Shah J, Kotnala R, Mohapatra S, KhanS A,ShahJ, KotnalaR, MohapatraS (2017). Nanostructured TiO_2 thin films prepared by RF magnetron sputtering for photocatalytic applications. Applied Surface Science, 422: 953– 961

Singh S, Barick K, Bahadur D (2011). Novel and efficient three dimensional mesoporous ZnO nanoassemblies for envirnomental remediation. International Journal of Nanoscience, 10(04/05): 1001–1005

Su C, Hong B Y, Tseng C M (2004). Sol-gel preparation and photocatalysis of titanium dioxide. Catalysis Today, 96(3): 119–126

Shi L, Liang L, Ma J, Meng Y, Zhong S, Wang F, Sun J (2014). Highly efficient visible light-driven Ag/AgBr/ZnO composite photocatalyst for degrading rhodamine B. Ceramics International, 40(2): 3495–3502

Sun Q, Lu Y, Yang D, Li J, Liu Y(2014). Preliminary observations of hydrothermal growth of nanomaterials on wood surfaces. Wood Science and Technology, 48(1): 51–58

Thomas M, Naikoo G A, Sheikh M U D, Bano M, Khan F (2016). Effective photocatalytic degradation of Congo red dye using alginate/carboxymethyl cellulose/TiO_2 nanocomposite hydrogel under direct sunlight irradiation. Journal of Photochemistry and Photobiology A Chemistry, 327: 33–43

Tian J, Zhao Z, Kumar A, Boughton R I, Liu H (2014). Recent progress in design, synthesis, and applications of one-dimensional TiO_2 nanostructured surface heterostructures: A review. Chemical Society Reviews, 43(20): 6920–6937

Tomita K, Petrykin V, Kobayashi M, Shiro M, Yoshimura M, Kakihana M (2006). A water-soluble titanium complex for the selective synthesis of nanocrystalline brookite, rutile, and anatase by a hydrothermal method. Angewandte Chemie International Edition, 45(15): 2378–2381

Tonda S, Kumar S, Kandula S, Shanker V (2014). Fe-doped and-mediated graphitic carbon nitride nanosheets for enhanced photocatalytic performance under natural sunlight. Journal of Materials Chemistry. A, Materials for Energy and Sustainability, 2(19): 6772–6780

Venkatakrishnan P, Karthik V (2019). Structural, morphological and mechanical properties of electroless Ni-B based alloy coatings. Materials Today: Proceedings.

Vinodgopal K, Kamat P V, Technology (1995). Enhanced rates of photocatalytic degradation of an azo dye using SnO_2/TiO_2 coupled semiconductor thin films. Environmental Science & Technology, 29 (3): 841–845

Wahab R, Ansari S, Kim Y, Seo H, Kim G, Khang G, Shin H S (2007). Low temperature solution synthesis and characterization of ZnO nano-flowers. Materials Research Bulletin, 42(9): 1640–1648

Wan C, Jiao Y, Li J (2017). TiO_2 Microspheres grown on cellulose-based carbon fiber: preparation, characterizations and photocatalytic activity for degradation of indigo carmine dye. Journal of Nanoscience and Nanotechnology, 17(8): 5525–5529

Wan C, Jiao Y, Li J (2016). Influence of pre-gelation temperature on mechanical properties of cellulose aerogels based on a green NaOH/PEG solution: A comparative study. Colloid & Polymer Science, 294 (8): 1281–1287

Wan C, Jiao Y, Liang D, Wu Y, Li J (2018). A geologic architecture system‐inspired micro‐/nano‐heterostructure design for high‐performance energy storage. Advanced Energy Materials, 8(33): 1802388

Wan C, Jiao Y, Wei S, Li X, Tian W, Wu Y, Li J (2019a). Scalable top-to-bottom design on low tortuosity of anisotropic carbon aerogels for fast and reusable passive capillary absorption and separation of organic leakages. ACS Applied Materials & Interfaces, 11(51): 47846–47857

Wan C, Jiao Y, Wei S, Zhang L, Wu Y, Li J (2019b). Functional nanocomposites from sustainable regenerated cellulose aerogels: A review. Chemical Engineering Journal, 359: 459–475

Wan C, Lu Y, Jiao Y, Jin C, Sun Q, Li J (2015a). Ultralight and hydrophobic nanofibrillated cellulose aerogels from coconut shell with ultrastrong adsorption properties. Journal of Applied Polymer Science, 132(24): 42037

Wan C, Lu Y, Jin C, Sun Q, Li J (2015b). A facile low-temperature hydrothermal method to prepare anatase titania/cellulose aerogels with strong photocatalytic activities for rhodamine B and methyl orange degradations. Journal of Nanomaterials, 2015: 1–8

Wang D, Xiao L, Luo Q, Li X, An J, Duan Y (2011a). Highly efficient visible light TiO_2 photocatalyst prepared by sol-gel method at temperatures lower than 300°C. Journal of Hazardous Materials, 192 (1): 150–159

Wang H, Bai Y, Wu Q, Zhou W, Zhang H, Li J, Guo L (2011b). Rutile TiO_2 nano-branched arrays on FTO for dye-sensitized solar cells. Physical Chemistry Chemical Physics, 13(15): 7008–7013

Wang H, Yuan X, Wu Y, Zeng G, Chen X, Leng L, Li H (2015a). Synthesis and applications of novel graphitic carbon nitride/metal-organic frameworks mesoporous photocatalyst for dyes removal. Applied Catalysis B: Environmental, 174-175: 445–454

Wang W J, Gao K H, Li Z Q (2016). Thickness-dependent transport channels in topological insulator Bi_2Se_3 thin films grown by magnetron sputtering. Scientific Reports, 6(1): 25291

Wang Y, Li T, Yao Y, Li X, Bai X, Yin C, Williams N, Kang S, Cui L, Hu L (2018). Dramatic enhancement of CO_2 photoreduction by biodegradable light-management paper. Advanced Energy Materials, 8(16): 1703136

Wang Y, Pei Y, Xiong W, Liu T, Li J, Liu S, Li B (2015b). New photocatalyst based on graphene oxide/chitin for degradation of dyes under sunlight. International Journal of Biological Macromolecules, 81: 477–482

Wang Y, Wang Q, Zhan X, Wang F, Safdar M, He J (2013). Visible light driven type II heterostructures and their enhanced photocatalysis properties: A review. Nanoscale, 5(18): 8326–8339

Wei S, Zeng C, Lu Y, Liu G, Luo H, Zhang R (2019). Degradation of antipyrine in the Fenton-like process with a La-doped heterogeneous catalyst. Frontiers of Environmental Science & Engineering, 13 (5):66 doi:10.1007/s11783-019-1149-9

Wong Y L, Tobin J, Xu Z, Vilela F (2016). Conjugated porous polymers for photocatalytic applications. Journal of Materials Chemistry. A, Materials for Energy and Sustainability, 4(48): 18677–18686

Wu L, Buchholz D, Bresser D, Gomes Chagas L, Passerini S(2014). Anatase TiO_2 nanoparticles for high power sodium-ion anodes. Journal of Power Sources, 251: 379–385

Xia P, Zhu B, Yu J, Cao S, Jaroniec M (2017). Ultra-thin nanosheet assemblies of graphitic carbon nitride for enhanced photocatalytic CO_2 reduction. Journal of Materials Chemistry, 5(7): 3230–3238

Xiao H, Zhang W, Wei Y, Chen L (2018). Carbon/ZnO nanorods composites templated by TEMPO-oxidized cellulose and photocatalytic activity for dye degradation. Cellulose, 25(3): 1809–1819

Xiong T, Cen W, Zhang Y, Dong F (2016). Bridging the g-C_3N_4 interlayers for enhanced photocatalysis. ACS Catalysis, 6(4): 2462–2472

Xu P, Yang J, Chen Y, Li Y, Jia X, Song H (2019). Wood-derived fiber/BiOBr/AgBr sponges by in situ synthesis for separation of emulsions and degradation of dyes. Materials & Design, 183: 108179

Xu Q, Zhang L, Yu J, Wageh S, Alghamdi A A, Jaroniec M (2018). Direct Z-scheme photocatalysts: principles, synthesis, and applications. Materials Today, 21(10): 1042–1063

Xuan L, Fu Y, Liu Z, Wei P, Wu L (2018). Hydrophobicity and photocatalytic activity of a wood surface coated with a Fe^{3+}-doped SiO_2/TiO_2 Film. Materials (Basel), 11(12): 2594

Yamashita H, Mori K, Kuwahara Y, Kamegawa T, Wen M, Verma P, Che M (2018). Single-site and nano-confined photocatalysts designed in porous materials for environmental uses and solar fuels. Chemical Society Reviews, 47(22): 8072–8096

Yu D H, Yu X, Wang C, Liu X C, Xing Y M (2012). Synthesis of natural cellulose-templated TiO_2/Ag nanosponge composites and photocatalytic properties. ACS Applied Materials & Interfaces, 4(5): 2781–2787

Yu Y, Xu D (2007). Single-crystalline TiO_2 nanorods: highly active and easily recycled photocatalysts. Applied Catalysis B: Environmental, 73(1–2): 166–171

Zangeneh H, Zinatizadeh A A L, Habibi M, Akia M, Hasnain Isa M (2015). Photocatalytic oxidation of organic dyes and pollutants in wastewater using different modified titanium dioxides: A comparative review. Journal of Industrial and Engineering Chemistry, 26: 1–36

Ebrahimzadeh M A , Mortazavi-Derazkola S , Zazouli M A (2019). Eco-friendly green synthesis and characterization of novel $Fe_3O_4/SiO_2/Cu_2O$-Ag nanocomposites using crataegus pentagyna fruit extract for photocatalytic degradation of organic contaminants. Journal of Materials Science Materials in Electronics, 30(12): 10994–11004

Zhang J, Zhou P, Liu J, Yu J (2014). New understanding of the difference of photocatalytic activity among anatase, rutile and brookite TiO_2. Physical Chemistry Chemical Physics, 16(38): 20382–20386

Zhang R, Wan W, Li D, Dong F, Zhou Y (2017). Three-dimensional MoS_2/reduced graphene oxide aerogel as a macroscopic visible-light photocatalyst. Chinese Journal of Catalysis, 38(2): 313–320

Zhang X, Qin J, Xue Y, Yu P, Zhang B, Wang L, Liu R (2015). Effect of aspect ratio and surface defects on the photocatalytic activity of ZnO nanorods. Scientific Reports, 4(1): 4596

Zhang Y, Zhang Y, Li X, Zhao X, Lyu X (2020). Photocatalytic water splitting of ternary graphene-like photocatalyst for the photocatalytic hydrogen production. Frontiers of Environmental Science & Engineering, 14(4):69

Zhao W, Wei Z, Ma L, Liang J, Zhang X (2019). Ag_2S quantum dots based on flower-like SnS_2 as matrix and enhanced photocatalytic degradation. Materials (Basel), 12(4): 582

Zhao Y, Zhao B, Liu J, Chen G, Gao R, Yao S, Li M, Zhang Q, Gu L, Xie J, Wen X, Wu L Z, Tung C H, Ma D, Zhang T (2016). Oxide-modified nickel photocatalysts for the production of hydrocarbons in visible light. Angewandte Chemie International Edition, 55(13): 4215–4219

Zhou C, Lai C, Huang D, Zeng G, Zhang C, Cheng M, Hu L, Wan J, Xiong W, Wen M, Wen X, Qin L (2018). Highly porous carbon nitride by supramolecular preassembly of monomers for photocatalytic removal of sulfamethazine under visible light driven. Applied Catalysis B: Environmental, 220: 202–210

Zhu K, Hu G (2014). Supercritical hydrothermal synthesis of titanium dioxide nanostructures with controlled phase and morphology. Journal of Supercritical Fluids, 94: 165–173

Zhu S, Wu Y, Chen Q, Yu Z, Wang C, Jin S, Ding Y, Wu G (2006). Dissolution of cellulose with ionic liquids and its application: A mini-review. Green Chemistry, 8(4): 325–327

Zhu Y, Huang L, Zou R, Zhang J, Yu J, Wu M, Wang J, Su Q (2016). Hydrothermal synthesis, morphology and photoluminescent properties of an Mn^{4+}-doped novel red fluoride phosphor elpasolite K_2LiAlF_6. Journal of Materials Chemistry. C, Materials for Optical and Electronic Devices, 4(24): 5690–5695

Zinatloo-Ajabshir S, Mortazaviderazkola S, Salavatiniasari M (2017). Schiff-base hydrothermal synthesis and characterization of Nd_2O_3 nanostructures for effective photocatalytic degradation of eriochrome black T dye as water contaminant. Journal of Materials Science Materials in Electronics, 28(23): 17849–17859

Zou J J, Liu C J, Yu K L, Cheng D G, Zhang Y P, He F, Du H Y, Cui L (2004). Highly efficient Pt/TiO_2 photocatalyst prepared by plasma-enhanced impregnation method. Chemical Physics Letters, 400(4–6): 520–523